NASA TECHNICAL NOTE

NASA TN D-6819

A VERSATILE MÖSSBAUER SPECTROMETER AND ITS APPLICATIONS IN VIBRATION MEASUREMENT

by Jag J. Singh and Lona M. Howser
Langley Research Center
Hampton, Va. 23365

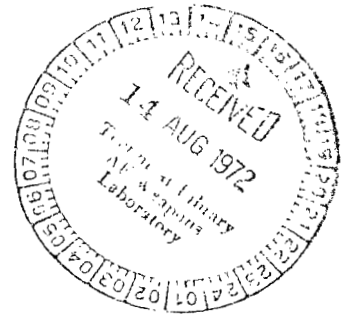

NATIONAL AERONAUTICS AND SPACE ADMINISTRATION • WASHINGTON, D. C. • AUGUST 1972

1. Report No.	2. Government Accession No.	3. Recipient's Catalog No.
NASA TN D-6819		

4. Title and Subtitle	5. Report Date
A VERSATILE MÖSSBAUER SPECTROMETER AND ITS APPLICATIONS IN VIBRATION MEASUREMENT	August 1972
	6. Performing Organization Code

7. Author(s)	8. Performing Organization Report No.
Jag J. Singh and Lona M. Howser	L-8318
	10. Work Unit No.
9. Performing Organization Name and Address	501-22-05-07
NASA Langley Research Center Hampton, Va. 23365	11. Contract or Grant No.
	13. Type of Report and Period Covered
12. Sponsoring Agency Name and Address	Technical Note
National Aeronautics and Space Administration Washington, D.C. 20546	14. Sponsoring Agency Code

15. Supplementary Notes

16. Abstract

A versatile Fe^{57}-Mössbauer spectrometer, equally efficient in transmission and reflection geometries, is described. The radiation detector consists of a 1.524- by 5.08- by 5.08-cm rectangular NaI(Tl) crystal with a hole 1.524 cm in diameter. The front and back faces of the crystal are covered with beryllium windows 0.0127 cm thick and 3.81 cm in diameter. The energy of the radiation accepted for counting ranges from 6.3 keV conversion X-rays to the 14.4 keV reemitted gamma rays. The spectrometer has been used to measure various types of low frequency (<10 Hz) and low amplitude (<0.254 mm) periodic motion of steel specimens.

17. Key Words (Suggested by Author(s))	18. Distribution Statement
Mössbauer spectrometer Scattering technique Vibration measurement	Unclassified – Unlimited

19. Security Classif. (of this report)	20. Security Classif. (of this page)	21. No. of Pages	22. Price*
Unclassified	Unclassified	40	$3.00

*For sale by the National Technical Information Service, Springfield, Virginia 22151

CONTENTS

A VERSATILE MÖSSBAUER SPECTROMETER AND ITS APPLICATIONS IN VIBRATION MEASUREMENT

By Jag J. Singh and Lona M. Howser
Langley Research Center

SUMMARY

The present study was undertaken in order to design, construct, and test a bench model of a Mössbauer spectrometer efficiently operable in the scattering mode. Such a spectrometer has been developed and used to perform experiments intended to demonstrate the applicability of Mössbauer-effect spectroscopy to important problems in structural mechanics without any special specimen preparation. One such experiment which dealt with the measurement of low frequency (<10 Hz) and low amplitude (<0.254 mm) periodic vibrations of austenitic steel specimens is described in detail. From these investigations, it is concluded that using the present spectrometer, measurements can be made on a variety of structural materials under environmental conditions without any special specimen preparation. The spectrometer system has been constructed almost entirely from commercially available components.

INTRODUCTION

In order to extend the applicability of the Mössbauer effect to nondestructive measurements in surface stress studies, structural vibration analysis, and liquid-solid interactions, it is essential to use reflection (backscattering) technique instead of the standard transmission method. Backscattering technique, however, has not yet been fully developed due to the special detector configuration requirements for a large solid angle at the surface under examination.

Several attempts at backscattering technique have been recently reported (refs. 1 to 4). These studies are based on the detection of either the reemitted 14.4 keV gamma rays or the 6.3 keV conversion X-rays or the conversion electrons. Although the Fe^{57}-backscattering technique should be most efficient when the low energy conversion electrons are detected, it is suitable for very thin surfaces (<3000 Å) only. Even for thin-surface studies, this technique requires that the specimen be kept in high vacuum and is further hampered by the limited penetrating power of the low-energy conversion electrons through the detector windows. A new Fe^{57}-radiation detector, which can subtend an angle as large as π steradians at the sample surface in both the transmission and the reflec-

tion geometries, has been designed and developed. The detector is relatively rugged in construction since it involves the detection of the reemitted 14.4 keV gamma rays and the 6.3 keV conversion X-rays.

The detector has been used in the measurement of low frequency (<10 Hz) and low amplitude (<0.254 mm) cyclic vibrations of austenitic steel specimens. When a Co^{57}-Pt source is moving with constant-acceleration motion, the Mössbauer spectrum from a stationary scatterer is characterized by a single peak centered at a certain source velocity p_0. If now the scatterer is subjected to low frequency, low amplitude periodic motion, which has no phase relationship with the source motion, conditions of Mössbauer resonance between the emitter and the absorber atoms can occur at any source velocity in the range of $p_0 \pm V_{max}$ where V_{max} represents the maximum scatterer velocity. This situation leads to a characteristically modified Mössbauer resonance peak from a moving scatterer. A comparison between the spectra from the stationary and the moving scatterers can then be used to infer the particulars of the scatterer motion. (Even though, by its very nature, the Mössbauer effect gives information about the relative motion of the source-absorber atoms, there have not been many applications of Mössbauer spectrometry to vibration analysis as such. The few reported techniques are of the contacting type, applicable over limited velocity ranges and depend upon the use of standard reference absorbers. (See refs. 5 and 6.) One such study (ref. 6) typically involved obtaining velocity calibration absorption spectra of various source-absorber combinations. The source-absorber combinations were subdivided into three cases: resonance, partial resonance, and off-resonance. All of these combinations involved attaching the Mössbauer source to the system under test and using standard-reference stationary absorbers in transmission geometry. Such measurements, besides involving source mounting adaptation, require electronic gating techniques to limit counting intervals to selected velocity ranges. In order to eliminate these requirements, a new, noncontacting, technique of adapting Mössbauer-effect spectroscopy to vibration measurements in materials containing Mössbauer nuclei has been developed. (See ref. 7 for the list of these nuclei.) This technique does not require any special specimen preparation, is applicable over a wide velocity range (submillimeter to several centimeters/second) and lends itself easily to determining the type of specimen-motion waveform. It has been applied to analyze the vibration of stainless steel specimens.) Results of several experiments involving different types of specimen motion and computer programs developed for analyzing the complex spectra, observed when the source and the scatterer are in random simultaneous motion, will be described.

SYMBOLS

A amplitude of Lorentzian peak

$I(x)$ observed counts in the channel centered at source velocity x (constant acceleration)

i index

$n = V_{max}/\Delta V$

p_o position of the Lorentzian peak on the source-velocity axis corresponding to zero scatterer velocity

$S_i = \frac{\Delta V}{dV/dt}$

t time

$V(t)$ scatter velocity at time t

V_{max} maximum value of the scatterer velocity

x source velocity

Γ full width of Lorentzian peak at half maximum intensity

ω angular velocity

Subscripts:

o,i indices

RADIATION DETECTOR AND ITS PERFORMANCE

The radiation detector consists of a 1.524- by 5.08- by 5.08-cm NaI(Tl) crystal with a central hole 1.524 cm in diameter. A sodium iodide scintillation crystal was chosen as the detector because of its high efficiency for low energy gamma (or X-) rays and easy availability in various geometrical shapes and sizes. The crystal encapsulation incorporates front and back beryllium windows 0.0127 cm thick and 3.81 cm in diameter, that permit easy penetration by the conversion X-rays and the reemitted 14.4 keV gamma rays into the sensitive region of the NaI(Tl) crystal. At the two ends the crystal is coupled, via quartz light guides, to two matched photomultipliers. Figure 1 shows a schematic drawing of the detector assembly. The electronic gains of the two photomultipliers are

equalized and the signals at the respective collectors are added and amplified before passing through a single channel analyzer (SCA). The limits of the SCA are set to accept all pulses in the range of 5 – 15 keV. Figure 2 shows a simplified diagram of the electronic circuit. The collimator assembly shown in figure 2(b) keeps the incident photon beam divergence at the scatterer to an angle less than 2.5°. This low divergence reduces the source velocity dispersion at the scatterer to less than 0.1 percent. The radiation counter, in combination with a sensitive electromechanical transducer and drive system producing motion of the source with constant acceleration through a range of velocities, has been used to study the Mössbauer spectra in both the transmission and reflection geometries.[1] Figures 3 and 4 show the transmission and the reflection spectra, respectively, obtained with a 0.8 mg/cm2, Fe^{57}-enriched iron target. Figure 5 shows a typical backscattered Mössbauer spectrum obtained with a 0.0762-cm thick, nonmagnetic stainless steel (type 347) scatterer. The Mössbauer source in all these studies, was a 10-millicurie Co^{57} source in platinum matrix. The absorber or scatterer in each case was positioned to subtend an angle of π steradian at the detector (see fig. 2(b)). This large solid angle, besides reducing the experimental run time, improves the signal-to-noise ratio in the spectrum since part of the background is independent of the solid angle subtended by the detector at the scatterer, that is, scattering at the collimator edges and surrounding shield. From the spectra shown in figures 3 and 4, it is clear that the present detector configuration is capable of producing equally good transmission and reflection Mössbauer spectra. The observed resolution in the present study is largely limited by the NaI(Tl) detector resolution for the 5 to 15 keV electromagnetic radiation.

For an efficient use of the Mössbauer spectrometer for various types of studies indicated earlier, a computer program for analyzing experimental spectra has been developed. In this program, the experimental spectra are least-squares fitted to a curve made up of a parabola and a series of Lorentzian peaks superimposed on it. (See ref. 8.) For those cases where the Lorentzian peaks were smeared – such as those obtained when the scatterer had a sinusoidal or constant acceleration motion – a modified version of the program, described later, was used.

APPLICATIONS

The Mössbauer spectrometer has been used in a number of studies in structural mechanics. One such study is described below. This study involved measurement of the bulk motion of steel specimens subjected to low frequency (<10 Hz) and low amplitude (0.254 mm) periodically varying velocities.[2] Three types of periodic motions were

[1]The velocity scale of the spectrometer was calibrated using a standard soft iron transmission Mössbauer spectrum.

[2]These limits were determined mainly by the source characteristics (strength and recoilless fraction) and the scatterer-detector solid-angle considerations in the present study.

imposed on the specimens using a standard laboratory waveform generator. The specimens were 0.0762- by 2.54- by 10.16-cm pieces of austenitic stainless steel (type 347), mounted vertically at the end of a horizontal shaft of an electromagnetic vibrator energized by the waveform generator. It was assumed that the specimen motion followed the generator waveform. Figure 6 shows a schematic drawing of the experimental setup used in this study. The scatterer was subjected to the following types of motion:

Sinusoidal motion: $V(t) = V_{max} \sin \omega t$

Constant-velocity motion: $V(t) = \pm V_{max}$

Constant-acceleration motion: $V(t) = \pm V_{max} \mp ft$

where f = Constant acceleration

and $+V_{max} \gtrless V(t) \gtrless -V_{max}$

During all these experiments the source was moving with a constant-acceleration motion in the velocity range of ±6(1.274) mm/sec. The various combinations of source-scatterer motions are illustrated in figure 7.

Scatterer Moving With Sinusoidal Motion

A backscattered Mössbauer spectrum from a stationary nonmagnetic stainless steel (type 347) specimen was first taken and is shown in figure 5. However, when the specimen is subjected to a sinusoidal motion, which has random phase relationship with the source motion, the resonance peak position p_o can fall anywhere between $p_o \pm V_{max}$ where V_{max} corresponds to the maximum value of the scatterer velocity along the direction of Co^{57}-source motion. Thus, by measuring the spread in the resonance peak position, the maximum velocity of the scatterer along the source-scatterer direction can be computed. An independent measurement of the frequency of the scatterer motion should then permit a determination of its displacement (amplitude). Figure 8 shows a typical Mössbauer spectrum obtained when both the source and the scatterer were in motion with random phase relationship. It is clear from this figure that the scatterer spends maximum time at a velocity close to the maximum value, as expected for a sinusoidal motion. (Fig. 8 also suggests the possibility of using this technique to determine the exact waveform of the scatterer motion.) Figure 8 and other similar spectra, shown in figure 9, corresponding to different scatterer velocities, were computer analyzed by least-squares fitting the observed data to an expression of the form

$$I(x) = (ax^2 + bx + c) + \sum_{i=1}^{2n} S_i \frac{A_o}{(p_i - x)^2 + (\Gamma/2)^2} \qquad (1)$$

where $p_i = p_o + i\frac{V_{max}}{n}$, S_i represents relative dwell times $\left(\frac{\Delta V}{dV/dt}\right)$ for various constant-velocity intervals (ΔV) in the range $\left(-V_{max} \rightarrow +V_{max}\right)$, and $n = \frac{V_{max}}{\Delta V}$. Figure 10 illustrates the graphical technique of calculating S_i. The computer program, used in this analysis, was a modified version of the basic program described in reference 8. The modifications, along with the solution of a sample case, are described in the appendix. A comparison between the values of $\pm V_{max}$, computed from the Mössbauer spectra and from the measured values of the frequency and amplitude of the scatterer motion is shown in figure 11 and summarized in table I. (The velocity was calculated assuming the scatterer motion to be sinusoidal in response to the input sine wave.) The agreement is quite good.

Scatterer Moving With Constant-Velocity Motion

The nonmagnetic stainless steel (type 347) scatterer was subjected to a constant-velocity[3] motion in the range ±3(1.274) mm/sec and backscattered Mössbauer spectra were taken, in the same manner as described previously, for a constant-acceleration source motion in the range ±6(1.274) mm/sec. Figure 12 shows typical spectra for this type of source and scatterer motions. Notice the appearance of two additional peaks on either side of the zero-scatterer-motion peak. Spectra shown in figure 12 and others corresponding to different values of scatterer velocities were least-squares fitted[4] to an expression of the following form:

$$I(x) = (ax^2 + bx + c) + \sum_{i=1}^{3} \frac{A_i}{\left(p_i - x\right)^2 + (\Gamma/2)^2} \qquad (2)$$

where

$$p_1 = p_{o,1} = p_o - V_{max}$$

and

$$p_3 = p_{o,2} = p_o + V_{max}$$

[3]The constant-velocity calibration was obtained using Mössbauer spectroscopic technique. (Direct measurement.)

[4]The computer program used in this analysis was essentially the same as that described in reference 8, except for the fact that there were three independent resonance peaks – instead of the usual one (nonmagnetic) or six (magnetic) for uniphase steel spectra. The outside peaks were least-squares fitted using a half-width value corresponding to a stationary scatterer whereas the central peak required a slightly larger value due to its velocity dispersion.

The scatterer velocity amplitude is obtained from the position of the two extreme peaks $p_{o,1}$ and $p_{o,2}$ as follows:

$$p_{o,1} = p_o - V_{max}$$

$$p_{o,2} = p_o + V_{max}$$

where p_o is the peak position for a stationary scatterer. (It is also the position of the central peak.)

The central peaks in figure 12 arise from the fact that the scatterer velocity goes through zero in the $(\pm V_{max} \rightarrow \mp V_{max})$ transition in a finite (i.e., nonzero) time. A comparison between the Mössbauer-computed and directly measured scatterer velocities is shown in figure 13 and is also summarized in table I. The agreement between the two sets of values is quite good.

Scatterer Moving With Constant-Acceleration Motion

If the nonmagnetic steel scatterer is subjected to a constant-acceleration motion simultaneously with the constant-acceleration source motion, and if there is no phase correlation between the two motions, the resultant backscattered Mössbauer spectrum is expected to be of the following form:

$$I(x) = (ax^2 + bx + c) + \sum_{i=1}^{2n} \frac{A_o}{(p_i - x)^2 + (\Gamma/2)^2} \tag{3}$$

where

$$p_i = p_o + i\,\frac{V_{max}}{n}$$

Equation (3) is identical to equation (1) if S_i were the same for all velocity intervals ΔV. The Mössbauer spectra for this combination of source and scatterer motions can be computer analyzed using the same program as that for sinusoidal motion described in the appendix.

Figure 14 shows an experimentally observed spectrum with the scatterer moving with constant-acceleration motion. A theoretically predicted spectrum under these conditions is shown by a solid line in this figure. It is obvious that the experiment and the theory do not agree in this case. The experimental spectrum indicates that the scatterer spends more time at or near extreme velocities than elsewhere. An examination of the waveform-generator output showed that it was distorted (see insert in fig. 15). The theoretical spectrum was then computed using an expression of the type given in equation (1)

with the S_i values approximate to the scatterer-motion waveform in the present case. The S_i values used are shown in figure 15. Figure 16 shows a comparison between the experimental and the theoretical spectra under these conditions. The agreement is reasonably good.

This exercise has demonstrated that it is possible to extract information about the scatterer-motion waveform from the Mössbauer spectra observed when both the source and the scatterer are in random relative motion. From the S_i values required to fit the observed spectra, one can reconstruct the scatterer-motion waveform. Conversely, Mössbauer-effect spectroscopy can serve as the basis of control circuitry for maintaining a desired scatterer waveform over long periods of time.

Figure 17 shows a theoretical modification superimposed on a nonresonant Mössbauer spectrum in order to indicate how $\pm V_{max}$ of the scatterer can be calculated from constant-acceleration scatterer-motion spectra. In this figure, the source and the scatterer motions had the following values:

Source velocity (constant acceleration) = ±6(1.274) mm/sec

Scatterer velocity (constant acceleration) = ±2(1.274) mm/sec

Notice the raised section in the central part of the parabola. The peak positions corresponding to $p_{o(beginning)}$ and $p_{o(end)}$ give a measure of V_{max} by the following relation:

$$V_{max} = \frac{p_{o(end)} - p_{o(beginning)}}{2}$$

CONCLUDING REMARKS

A radiation-counter configuration suitable for reflection Mössbauer spectroscopy has been described. An application of the spectrometer, involving measurement of periodic vibrations of steel specimens has been discussed. The measured and the computed values are in agreement within the expected limits of errors. The errors on the computed values range from 0.7 percent to 3.0 percent in the case of sinusoidal motion and 0.4 percent to 1.6 percent in the case of constant-velocity motion. The major source of error in the computed values lies in the statistical accuracy of determining the extreme scatterer-velocity points in the Mössbauer spectra. This error can be reduced by using a stronger source (i.e., 100 millicuries Co^{57} or stronger) which will also have a further desirable effect of reducing the experimental time correspondingly.

Langley Research Center,
National Aeronautics and Space Administration,
Hampton, Va., June 21, 1972.

APPENDIX

MODIFICATION OF THE COMPUTER PROGRAM DESCRIBED IN REFERENCE 8 TO ALLOW FOR THE EFFECTS OF SCATTERER MOTION AND A SAMPLE CASE

Computer Program

The basic computer program D3290 developed at Langley Research Center to analyze a complex Mössbauer spectrum from a stationary scatterer has been described in detail in reference 8. This program has been slightly modified to include the effects of scatterer motion in the present study. The modified program D3291 least-squares fits the observed spectrum to an expression of the form given in the text in equation (1), which describes a parabola plus a series of gradually displaced Lorentzian peaks. The instructions for the use of program D3291 are the same as for the basic program D3290 except for a few additions. These additions and modifications are described below.

The program D3291 is run as if there was a single peak. The input NP = 1 and the dimensions have been reduced to allow for only one peak. Three new inputs are required and two inputs are redefined. An additional variable is printed with the output and two are redefined. These are listed below:

New Input

FORTRAN variable	Dimension	Description
CGAMO	(1)	Peak width at half maximum intensity, set equal to the half-width value for a stationary scatterer. (D3290 gives the value for a stationary scatterer.)
NDT		Number of subdivisions of the velocity cycle
PO	(1)	Initial estimate for $p_o - V_{max}$
P20	(1)	Initial estimate for $p_o + V_{max}$
RT	(1300)	Relative dwell times, S_i

New Output

Heading	Description
P	Position of $(p_o - V_{max})$ on the velocity axis
P2	Position of $(p_o + V_{max})$ on the velocity axis
CGAM	Peak width at half maximum intensity

The results given in this report were obtained by dividing the scatterer motion into 1248 subdivisions. This number was selected to ensure that the corresponding V_{max} had saturated to its true value within the limits of accuracy of the present system. The program can be altered to find an optimum number of subdivisions for a given experimental system.

Program D3291 requires approximately 60 000 octal locations of core storage. A typical case using 1248 displaced Lorentzian peaks runs in 400 seconds.

The listing for program D3291 is as follows:

```
      PROGRAM D3291 (INPUT=201,OUTPUT= 201,TAPE5=INPUT,TAPE6=OUTPUT,
     1 SCFILE,TAPE7=SCFILE)
      COMMON A(1),A0(1),AREA(1),ARRAY(1025,7),B(7,8),C(7,1),CGAM(1),
     2 CGAM0(1),ERROR(7),P(1),P0(1),P2(1),P20(1),P(1025),RT(1300),
     2 RS(650),X(1025),Y(1025)
      DIMENSION COMPY(1025),PAR(1025),YYPAR(2050)
      DIMENSION PRM(3),XM(3),YM(2)
      EQUIVALENCE (PRM(1),SA0),(PRM(2),BC),(PRM(3),C0)
      EQUIVALENCE (COMPY(1),ARRAY(1,1))  ,(PAR(1),ARRAY(1,2))
      EQUIVALENCE (YYPAR(1),ARRAY(1,3))
      DIMENSION IPIVOT (21),INDEX(21,2)
      EQUIVALENCE (R(1),IPIVOT(1)),(R(22),INDEX(1,1))
      DIMENSION V(7,7)
      EQUIVALENCE (V(1,1),ARRAY(1,4))
      NAMELIST /NAM1/ A0,B0,CGAMC,ERROR,IERR,IFLAG,IPRINT,NDT,NP,P0,P20,
     1 PT,SA0,VELB
      DATA XM,YM/27H SOURCE VELOCITY   (MM/SEC),19H COUNTS PER CHANNEL/
      NRC=7
      CALL CALCOMP
      CALL LEROY
      CON=1
    2 READ (5,NAM1)
      IF (EOF,5) 3,4
    3 CALL CALPLT (0,0,999)
      STOP
    4 CONTINUE
      CGAM(1)=CGAM0(1)
C INTERPOLATE, GET MORE DWELL TIMES
      N1=40
    5 CONTINUE
      DO 6 I=1,N1
    6 RS(I)=RT(I)
      DO 7 I=2,N1
      K=2*I -1
      RT(K-1) =( RS(I-1) + RS(I))/2.
    7 RT(K)=RS(I)
      N1=K
      IF (N1 .LT.NDT)  GO TO 5
      NDT=K
      ANDT=K
      IF (IFLAG.NE.1) GO TO 27
      READ (5,9) ID,NC
```

```
    9 FORMAT (5X,I5,I10)
      IF (NO) 10,12,12
   10 NO=-NO
      CON=-1
   11 FORMAT (8(F4.0,F6.0))
   12 READ (5,11) (X(I),Y(I),I=1,NO)
C SCAN ARRAY AND INTERPOLATE FOR BAD POINTS
      J=1
      DO 18 I=2,NO
      IF (Y(I).EQ.0.) GO TO 16
      IF (J.EQ.1) GO TO 18
      FAC= (Y(I)-Y(K))/J
      J=J-1
      DO 13 N=1,J
   13 Y(K+N)=Y(K-1+N)+ FAC
      J=1
      GO TO 18
   16 IF (J.EQ.1) K=I-1
      J=J+1
   18 CONTINUE
      REWIND 7
      WRITE (7) (Y(I),I=1,NO)
      CO=Y(1)
      ANO=NO-1
      X1=X(1)
      SUM = VELB *2.
      DO 21 I=1,NO
      X(I)= (VELB-SUM* (X(I)-X1)/ANO) *CON
   21 CONTINUE
   27 ITER=0
      WRITE (6,2700) ID,IERR
 2700 FORMAT (*1CASE NO.*I5,5X*IERR=*I3)
      IF (IERR.EQ.1) GO TO 32
      REWIND 7
      READ (7) (Y(I),I=1,NO)
      GO TO (32,28,29),IERR
   28 DO 2810 I=1,NO
      Y(I)=Y(I)+ SQRT(Y(I))
 2810 CONTINUE
      GO TO 32
   29 DO 2910 I=1,NO
      Y(I)=Y(I)- SQRT(Y(I))
 2910 CONTINUE
   32 DO 40 I=1,NO
      XSQ=X(I)**2
      ARRAY(I,1)=XSQ
      ARRAY(I,2)= X(I)
      ARRAY(I,3)=1.
      FX= SAC*XSQ + BO*X(I)+ CO
      R(I)=(Y(I)- FX)
   40 CONTINUE
   80 NP3=3*NP +3
      N1=NP3+1
C INITIALIZE PLOT ROUTINE AND SET ORIGIN
      MM=4
      DO 110 M=1,NP
      SAVE=CGAMC(M)**2 /4.0
      SAVE1=AO(M)* CGAMO(M)/2.0
      A2= 2.0 *AC(M)
      P6= (P2C(M)-PC(M))/ ANDT
```

```
      DO 100 I=1,NO
      PMX= PO(M) - X(I)
      SA=0.0
      SP=0.0
      SG=0.0
      SP2=0.0
      DO 90 J=1,NDT
      PNUM= PMX +J*P6
      DENOM=PNUM **2 + SAVE
      DSQ= DENOM*DENOM
      SA=SA + RT(J) /DENOM
      SG= SG - RT(J)*SAVE1 /DSQ
      AJ=J/ANDT
      PART=RT(J)*A2*PNUM/DSQ
      SP=SP -PART*(1.-AJ)
      SP2=SP2- PART*AJ
   90 CONTINUE
      ARRAY(I,MM)=SA
      ARRAY(I,MM+1) =SP
      ARRAY(I,MM+2) =SP2
      FX= AO(M) *ARRAY(I,MM)
      R(I)=R(I)-FX
  100 CONTINUE
      MM=MM+3
  110 CONTINUE
C ARRAY TRANSPOSE * ARRAY
      DO 120 K=1,NP3
      DO 118 M=1,NP3
      B(K,M)=0.0
      DO 115 I=1,NO
      B(K,M)=ARRAY(I,K)*ARRAY(I,M) + B(K,M)
  115 CONTINUE
  118 CONTINUE
  120 CONTINUE
C  ARRAY TRANSPOSE * R
      DO 129 K=1,NP3
      C(K)=0.0
      DO 125 M=1,NO
  125 C(K)=ARRAY(M,K)*R(M) + C(K)
  129 CONTINUE
      CALL MATINV (B,NP3,C,1,DET,IPIVOT, INDEX,7 ,ISCALE)
      ITER=ITER+1
      DO 142 I=1,3
      TEST1= ABS(C(I)/PRM(I))
      IF (TEST1.GT.EPROR(I)) GO TO 800
  142 CONTINUE
      MM=4
      DO 145 M=1,NP
      TEST1= ABS(C(MM)/AO(M))
      IF (TEST1.GT.ERROR(MM)) GO TO 800
      TEST1= ABS(C(MM+1)/PO(M))
      IF (TEST1.GT.ERROR(MM+1)) GO TO 800
      TEST1= ABS(C(MM+2)/ P2O(M))
      IF (TEST1.GT.ERROR(MM+2)) GO TO 800
  145 CONTINUE
  165 MM=4
      SAO=SAO+ C(1)
      BO=BO+C(2)
      CO=CO + C(3)
```

```
      DO 168 M=1,NP
      A(M)= C(MM)+ AC(M)
      P(M)= C(MM+1) + PO(M)
      P2(M)=C(MM+2) + P2O(M)
      MM= MM+3
  168 CONTINUE
      DO 170 I=1,NO
      R(I)=Y(I)
  170 COMPY(I)=0.0
      DO 174 M=1,NP
      P6= (P2C(M)- PC(M))/ ANDT
      SAVE= CCAM(M)**2/4.0
      DO 172  I=1,NO
      PMX=P(M)-X(I)
      DO 171 J=1,NDT
      D    =P6*J
      PEAK    =RT(J)*A(M)/((PMX+D    )**2+SAVE)
      COMPY(I)=COMPY(I)+ PEAK
  171 CONTINUE
  172 CONTINUE
  174 CONTINUE
      DO 176 I=1,NO
      PAR(I)= SAO*X(I)**2 + BO*X(I) +CO
      COMPY(I)= COMPY(I) + PAR(I)
  176 R(I)=R(I)-COMPY(I)
      STD=0.0
      DO 178 I=1,NO
  178 STD=R(I)**2+ STD
      ANN=NO-NP3
      STD=STD/ANN
      DO 181 I=1,NP3
      DO 180 J=1,NP3
      V(I,J)=B(I,J)*STD
  180 CONTINUE
  181 CONTINUE
      DO 183 I=1,NP3
  183 V(I,1)=SQRT(V(I,I))
      STD=SQRT(STD)
      P1=VELB**3/3.
      P3=VELB**2/2.
      AR1=SAO*P1 + BO*P3 + CO*VELB
      AR2= -SAO*P1 + BO*P3 - CO*VELB
      AREA1= AR1 - AR2
      AREA2=0.
      WRITE (6,185) SAO,V(1,1),BO,V(2,1),CO,V(3,1),ITER
  185 FORMAT (48HOCOEFFICIENTS OF PARABOLA    Y= SA*X**2 + B*X + C/      *
     1 SA=*E15.8, *(T*E9.3,*)*,5X*B=*E15.8, *(T*E9.3,*)*,5X,*C=*E15.8,
     2 *(T*E9.3,*)*/
     3         1H+,19X,1H-,33X,1H-,33X,1H-/*0NO. OF ITERATIONS=*I6)
      DO 200 M=1,NP
C
C EVALUATE INTEGRALS TO GET AREAS FOR PHI2
C
      SAVE=CCAM(M)**2/4.0
      P6= (P2(M)-P(M)) /ANDT
      DO 191 J=1,NDT
      C1= A(M)*RT(J)
      AJ=J
      C2 = SAVE +P(M)**2+ 2.0*P(M)* AJ*P6+ (AJ*P6)**2
```

```
      AC=C2
      BC=-2.0 *(AJ*P6+ P(M))
      CC =  1.0
      Q = 4.0 *AC*CC  -BC**2
      IF  (Q ) 186,940,187
  186 FAC = 12.*CC +  BC
      FAC1= SQRT (- Q)
      FAC2= (FAC - FAC1) /(FAC + FAC1)
      FAC =ALOG (FAC2)
      AR1 = FAC / FAC1
      FAC = -12. *CC + BC
      FAC2= (FAC -FAC1)/ (FAC + FAC1)
      FAC = ALOG (FAC2)
      AR2 = FAC/ FAC1
      AREA(M)=(AR1- AR2) *C1
      AREA2= AREA(M) + AREA2
      GO  TO 189
  187 FAC1= SQRT (Q)
      FAC =(12.0*CC + BC )
      FAC2=ATAN2(FAC,FAC1)
      AR1 = 2.C * FAC2 / FAC1
      FAC =(-12.0*CC +BC )
      FAC2=ATAN2(FAC,FAC1)
      AR2 = 2.0* FAC2/ FAC1
      AREA(M)=(AR1- AR2) *C1
      AREA2= AREA(M) + AREA2
  189 CONTINUE
  191 CONTINUE
      PHI2=ABS(AREA2/AREA1)
      AIS=P(M)
      WRITE (6,190) M
  190 FORMAT (*0PARAMETERS FOR PEAK*I3)
      WRITE (6,195) AIS
  195 FORMAT (*0IS=*E15.8)
      MS=3*M
      V(MS+4)=C.
      WRITE (6,205) A(M),V(MS+1),P(M),V(MS+2),P2(M),V(MS+3),CGAM(M),
     1 V(MS+4)
      WRITE (6,204)
  200 WRITE (6,203) AREA(M)
  203 FORMAT (*0AREA=*E13.6)
  204 FORMAT (1H+,16X,1H-,31X,1H-,32X,1H-,34X,1H-)
  205 FORMAT (*0A=*E13.6, *(T*E9.3,*)*,5X*P=*E13.6, *(T*E9.3,*)*5X*P2=*
     1 E13.6, *(T*E9.3,*)*, 5X*CGAM=*E13.6, *(T*E9.3,*)*  )
C    EVALUATE THESE PARAMETERS IF ONLY ONE PEAK
      YMAX=SAC*P(M)**2 + BO*P(M) + CC
      PHI1=A(M)/YMAX
      PDP=PHI1/PHI2
      WRITE (6,206) PHI1,PHI2,PDP
  206 FORMAT (*0PHI1=*E15.8,5X*PHI2=*E15.8,5X*PHI1/PHI2=*E15.8)
  210 IF (IPRINT. EQ.0) GO TO 380
      WRITE (6,230)
  230 FORMAT (*0CHANNEL NO.*3X*X MM/SEC*14X*Y*14X*COMPUTED Y*10X
     1 *RESIDUALS*10X*PARABOLA*)
      DO 315 I=1,NO
      WRITE (6,312) I,X(I),Y(I),COMPY(I),R(I)  ,PAR(I)
  312 FORMAT (I6,5E20.8)
  315 CONTINUE
      WRITE (6,370) STD
  370 FORMAT (*0STD=*E15.6)
```

APPENDIX – Continued

```
  380 K=1
      IF (IERR.NE.1) GO TO 2
C COMPUTE MINIMUMS AND MAXIMUMS
      XPG=12.
      CALL ASCALE (X,XPG,NO,K,10.)
      YPG=10.
      NUM=2*NO
      DO 400 I=1,NO
  400 YYPAR(I)=Y(I)
      N1=NO+1
      DO 410 I=  N1,NUM
  410 YYPAR(I)=PAR(I-NO)
      CALL ASCALE (YYPAR,YPG,NUM,K,10.)
      NP1=NO+1
      NP2=NO+2
      Y(NP1)=YYPAR(NUM+1)
      Y(NP2)=YYPAR(NUM+2)
      PAR(NP1)=Y(NP1)
      PAR(NP2)=Y(NP2)
      COMPY(NP1)=Y(NP1)
      COMPY(NP2)=Y(NP2)
C DRAW X AXIS
      XDV=10.
      XTIC=1.
      CALL AXES (0.,0.,0.,XPG,X(NP1),X(NP2),XTIC,XDV,XM,.15,-27)
C DRAW Y AXIS
      YDV=10.
      YTIC=1.
      CALL AXES (0.,0.,90.,YPG,COMPY(NP1),COMPY(NP2),YTIC,YDV,YM,.15,19)
C
C PLOT CURVE
C
      CALL PLPT (X,Y,NO)
      IF (ITER.GE.30 )GO TO 600
      CALL LINPLT (X,COMPY,NO,K,0,0,0,0)
      CALL LINPLT (X,PAR,NO,K,0,0,0,0)
C ESTABLISH A NEW REFERENCE POINT FOR THE NEXT GRAPH
  600 CALL CALPLT (14.,0.,-3)
      GO TO 2
  800 MM=4
      IF (ITER.GE.30) GO TO 1000
      DO 900 M=1,NP
      AO(M)= C(MM)+ AO(M)
      PO(M)=C(MM+1) + PO(M)
      P2O(M)=C(MM+2) + P2C(M)
  895 MM=MM+3
  900 CONTINUE
  920 SAO=SAO+ C(1)
      BO= BO+ C(2)
      CO =CO+ C(3)
      GO TO 32
  940 WRITE  (6,950) A,P,CGAM
  950 FORMAT (*0WHEN EVALUATING THE INTEGRALS Q EQUALS 0., THIS CANNOT
     1 BE, A,P,CGAM ARRAYS FOLLOW */(7E18.6))
      GO TO 2
 1000 DO 1020 I=1,NO
 1020 PAR(I)=Y(I)
      GO TO 380
      END
```

Sample Case

The input and output for a sample case are printed below. In this case, the source was moving with a constant acceleration in a velocity range of ±6(1.274) mm/sec. At the same time, but with no phase correlation with the source motion, the scatterer was undergoing a sinusoidal motion in the range of $\pm V_{max}$ = (1.16 ± 0.01) mm/sec. The source and the scatterer motions were collinear. The computer printout does not include a velocity calibration factor of 1.274.

The input for the sample case is as follows:

```
$NAM1 IFLAG=1,  IPRINT=0,  IERR=1,  SAO=50.,  BO=-5.,  ERROR=2*1.E-5,1.E-2,
  3*1.E-5,
  NP=1,  AO=.3,  PO=-1.1,  P2O=.6,  CGAMO=.2929,  VELB=6.,  NDT=1248,
   RT=.95,.35,.285,.25,.225,.205,.19,.175,.17,.165,.16,.155,.151,.15,.149,.146,
    .145,.141,.14,.139,
  .139,.14,.141,.145,.146,.149,.15,.151,.155,.16,.165,.17,.175,.19,.205,.225,
    .25,.285,.35,.95,
   $
        4      -1004
  2 37200    3 37214    4 37211    5 37557    6 36875    7 37155    8 37092    9 36589
 10 36978   11 37096   12 37016   13 36710   14 36787   15 36930   16 37214   17 36369
 18 36770   19 36778   20 37274   21 36937   22 36988   23 37161   24 36931   25 37211
 26 37017   27 37057   28 36934   29 36865   30 36541   31 36891   32 36836   33 36626
 34 36389   35 36500   36 36500   37 36554   38 36653   39 36996   40 36709   41 36724
 42 36419   43 36944   44 37000   45 36842   46 36624   47 37000   48 36694   49 36700
 50 36779   51 36500   52 36493   53 36712   54 37000   55 36923   56 36712   57 36731
 58 36513   59 36587   60 36053   61 36415   62 36834   63 36557   64 36571   65 36494
 66 36663   67 36659   68 36676   69 36777   70 36596   71 36979   72 36711   73 36600
 74 36620   75 36710   76 36637   77 36600   78 36630   79 36662   80 36472   81 36887
 82 36641   83 36339   84 36812   85 36601   86 35996   87 36115   88 36843   89 36858
 90 36485   91 36585   92     0   93 36255   94 36546   95 36535   96 36449   97 36320
 98 36796   99 36630 100 36679 101 36435 102 36080 103 36467 104 36551 105 36223
106 36498 107 36377 108 36356 109 36655 110 36302 111 36316 112 36272 113 36245
114 36126 115 36258 116 36199 117 36546 118 36470 119 36414 120 36489 121 36498
122 36129 123 36225 124 36293 125 36170 126 36368 127 36466 128 35973 129 35989
130 36344 131 36275 132 36192 133 36297 134 36463 135 36478 136 36069 137 36171
138 36540 139 36445 140 36007 141 36419 142 35928 143 36283 144 36160 145 36208
146 35948 147 36012 148 36473 149 36469 150 36259 151 36082 152 36212 153 36028
154 36347 155 36092 156 35915 157 36583 158 35875 159 36388 160 36030 161 35929
162 36203 163 36114 164 36125 165 36050 166 35952 167 35918 168 36088 169 36317
170 36269 171 35642 172 35897 173 36471 174 35749 175 35825 176 36121 177 36398
178 36085 179 36301 180 35858 181 36254 182 35665 183 36249 184 36291 185 35651
186 35853 187 36000 188 35991 189 35986 190 36032 191 35854 192 35684 193 36025
194 36045 195 36168 196 36356 197 36031 198 35885 199 35800 200 35895 201 35781
202 35828 203 36094 204 35968 205 36108 206 36244 207 36043 208 36109 209 35880
210 35741 211 35705 212 36052 213 35832 214 35718 215 35850 216 35916 217 36000
218 36000 219 35719 220 35844 221 35634 222 35542 223 35585 224 35704 225 36055
226 35923 227 35796 228 35985 229 35707 230 35631 231 35822 232 35603 233 35697
234 35917 235 35615 236 35901 237 35759 238 35933 239 35773 240 36014 241 35496
242 35975 243 35775 244 35794 245 35825 246 35447 247 35662 248 36054 249 35488
250 35895 251 35972 252 35670 253 35510 254 35850 255 36148 256 35793 257 35789
258 35563 259 35672 260 35833 261 35569 262 35784 263 35952 264 35880 265 35887
266 35366 267     0 268 35565 269 36012 270 35655 271 35584 272 35954 273     0
274 35704 275 35441 276 35666 277 35654 278 35824 279     0 280 35572 281 35686
282 35831 283 35859 284 35618 285 35577 286 35816 287 35911 288 35757 289 35740
290 35674 291 35436 292 35685 293 35600 294 35727 295 36046 296 35479 297 36030
298 35773 299 35416 300 35404 301 35529 302 35511 303 35494 304 35759 305 35852
306 35523 307 35829 308 35762 309 35671 310 35541 311 35789 312 35239 313 35886
```

314	35598	315	35524	316	35713	317	35756	318	35426	319	35305	320	35562	321	35584
322	35438	323	35524	324	35153	325	35663	326	35670	327	35587	328	35336	329	35565
330	35795	331	35581	332	35546	333	35452	334	35733	335	35677	336	35571	337	35723
338	35702	339	35668	340	35631	341	35543	342	35463	343	35420	344	35424	345	35292
346	35392	347	35499	348	35689	349	35597	350	35386	351	35483	352	35681	353	35442
354	35471	355	35663	356	35471	357	35672	358	35715	359	35238	360	35279	361	35561
362	35453	363	35492	364	35710	365	35763	366	35527	367	35678	368	35539	369	35598
370	35528	371	35308	372	35466	373	35225	374	35574	375	35641	376	35091	377	35320
378	35616	379	35080	380	35398	381	35643	382	35761	383	35770	384	35774	385	35897
386	35458	387	35479	388	35913	389	35706	390	35756	391	35882	392	35473	393	35577
394	35955	395	35961	396	35588	397	35919	398	36012	399	35658	400	35979	401	35924
402	36067	403	36097	404	35884	405	36117	406	35925	407	35880	408	36093	409	36102
410	36294	411	36001	412	36392	413	36273	414	35799	415	36037	416	36233	417	35993
418	35993	419	36063	420	36247	421	36104	422	36484	423	36264	424	36227	425	36070
426	36107	427	36390	428	36098	429	35981	430	36206	431	36030	432	36186	433	35886
434	36099	435	36245	436	36119	437	35948	438	36210	439	36268	440	36247	441	36158
442	36114	443	35985	444	36277	445	36218	446	36199	447	35950	448	36108	449	36119
450	36030	451	36217	452	35792	453	35898	454	36311	455	35997	456	36119	457	35914
458	36095	459	36190	460	36069	461	36179	462	35917	463	35995	464	35926	465	35718
466	36202	467	35866	468	36021	469	36119	470	35987	471	36057	472	36457	473	36050
474	35812	475	36194	476	36027	477	36197	478	35871	479	35738	480	35846	481	35901
482	36062	483	36287	484	36238	485	35961	486	35883	487	35846	488	35719	489	36067
490	36277	491	35961	492	35900	493	36203	494	35772	495	35777	496	35925	497	35898
498	35813	499	36165	500	35919	501	36033	502	35885	503	36279	504	35993	505	35891
506	36015	507	36103	508	35668	509	35784	510	35548	511	36113	512	35911	513	35598
514	36245	515	35887	516	36158	517	35814	518	36062	519	35994	520	35966	521	35847
522	36362	523	36089	524	35870	525	36043	526	36288	527	35991	528	36084	529	35884
530	35898	531	36109	532	36100	533	35857	534	36114	535	36060	536	36296	537	36369
538	36044	539	36282	540	36042	541	36086	542	36125	543	36168	544	36163	545	36059
546	36375	547	36172	548	36118	549	35986	550	35829	551	36217	552	36011	553	36084
554	35979	555	35931	556	36035	557	35788	558	35808	559	35600	560	35887	561	36066
562	35831	563	36116	564	35710	565	35570	566	35640	567	35922	568	35609	569	35667
570	35944	571	35597	572	35420	573	35663	574	35317	575	35804	576	35560	577	35600
578	35436	579	35287	580	35305	581	35542	582	35608	583	35576	584	35609	585	35328
586	35715	587	35334	588	35708	589	35249	590	35182	591	35486	592	35444	593	35648
594	35382	595	35434	596	35153	597	34981	598	35276	599	35631	600	35646	601	35355
602	35248	603	35455	604	35338	605	35615	606	35468	607	35563	608	35374	609	35486
610	35687	611	35192	612	35752	613	35258	614	34962	615	35573	616	35704	617	35126
618	35329	619	35979	620	35386	621	35506	622	35178	623	35216	624	35612	625	35192
626	35359	627	35322	628	35429	629	35572	630	35460	631	35428	632	35393	633	35253
634	35566	635	35314	636	35530	637	35359	638	35597	639	35494	640	35551	641	35587
642	35175	643	35465	644	35388	645	35594	646	35562	647	35560	648	35739	649	35341
650	35028	651	35647	652	35651	653	35526	654	35710	655	35374	656	35535	657	35303
658	35380	659	35769	660	35451	661	35633	662	35570	663	35695	664	35542	665	35322
666	35661	667	35418	668	35437	669	35645	670	35562	671	35962	672	35715	673	35478
674	35526	675	35603	676	35639	677	35436	678	35873	679	35822	680	35546	681	35479
682	35799	683	36071	684	35567	685	35692	686	35585	687	35613	688	35524	689	35653
690	35607	691	35390	692	35370	693	35875	694	35629	695	35417	696	35576	697	35819
698	35689	699	35758	700	35610	701	35989	702	35435	703	35447	704	35710	705	35446
706	35523	707	35530	708	35659	709	35347	710	35438	711	35536	712	35584	713	35786
714	35541	715	35686	716	35731	717	35673	718	35569	719	35902	720	35785	721	35817
722	35478	723	35376	724	35540	725	35548	726	35754	727	35515	728	35386	729	35501
730	36091	731	35574	732	35695	733	35448	734	35454	735	35816	736	35565	737	35965
738	35571	739	35434	740	35579	741	36056	742	35526	743	35852	744	35483	745	36074
746	35997	747	35456	748	35518	749	35576	750	35455	751	35677	752	35504	753	35665
754	35800	755	35919	756	35920	757	35472	758	35833	759	35939	760	35528	761	35740
762	35794	763	35573	764	35898	765	35782	766	35758	767	35956	768	36404	769	35840
770	35798	771	35655	772	35669	773	35864	774	35971	775	35653	776	35692	777	35902
778	35291	779	35728	780	35516	781	35698	782	35672	783	35912	784	35941	785	35621
786	35960	787	35914	788	35516	789	35936	790	35904	791	36293	792	35705	793	35723
794	35447	795	35906	796	36073	797	35840	798	35832	799	35885	800	35689	801	35614
802	35823	803	35798	804	35745	805	36020	806	36039	807	36007	808	36209	809	35764

810	35812	811	35936	812	36233	813	35828	814	35798	815	35723	816	35897	817	35966
818	36092	819	36055	820	36289	821	35651	822	35976	823	36106	824	36359	825	35807
826	36094	827	36576	828	35896	829	36099	830	36000	831	36275	832	35977	833	36064
834	35902	835	36062	836	36210	837	36186	838	36144	839	36299	840	35943	841	35964
842	36004	843	36120	844	36340	845	36226	846	35857	847	36166	848	36265	849	36221
850	36264	851	36025	852	36384	853	36167	854	36208	855	36107	856	36174	857	35952
858	36125	859	36180	860	35935	861	36000	862	35916	863	36140	864	36018	865	36402
866	35893	867	36578	868	36542	869	35955	870	36064	871	36324	872	36061	873	36082
874	36253	875	36207	876	36703	877	35984	878	36167	879	35912	880	36159	881	36441
882	36198	883	36257	884	35990	885	36410	886	35938	887	36358	888	35997	889	36123
890	36155	891	36121	892	36180	893	36014	894	36139	895	36243	896	36582	897	36466
898	36601	899	36435	900	36187	901	36332	902	36339	903	36359	904	36518	905	36487
906	36433	907	36282	908	36335	909	36007	910	36217	911	36503	912	36412	913	36366
914	36557	915	36732	916	36505	917	36191	918	36571	919	36695	920	36333	921	36243
922	36526	923	36411	924	36603	925	36274	926	36398	927	36955	928	36542	929	36500
930	36617	931	36427	932	36673	933	36509	934	36545	935	36236	936	36582	937	36866
938	36607	939	36534	940	36476	941	36511	942	36498	943	36464	944	36603	945	36556
946	36397	947	36782	948	36692	949	36463	950	36621	951	36435	952	36432	953	36717
954	36687	955	36492	956	36483	957	36951	958	36991	959	36490	960	36599	961	36873
962	36793	963	36768	964	36586	965	36664	966	36936	967	36508	968	36599	969	37250
970	36894	971	36612	972	36839	973	36558	974	37056	975	36678	976	36874	977	36707
978	36899	979	36772	980	36806	981	36722	982	36903	983	36682	984	36767	985	36884
986	36852	987	36536	988	37099	989	36599	990	36899	991	36742	992	36637	993	36778
994	36891	995	37164	996	37081	997	37283	998	37335	999	367931000		368221001		37020
1002	366641003		369911004		369711005		36812								

The output for the sample case is as follows:

```
CASE NO.     4      IERR=  1

COEFFICIENTS OF PARABOLA    Y= SA*X**2 + B*X + C
SA= 4.64546504E+01(∓6.579E-01)      B=-5.17809394E+00(∓1.699E+00)      C= 3.53220824E+04(∓1.210E+01)

NO. OF ITERATIONS=      8

PARAMETERS FOR PEAK  1

IS=-1.15833081E+00

A= 3.036201E-01(∓8.663E-03)      P=-1.158331E+00(∓1.646E-02)      P2= 6.092466E-01(∓1.647E-02)      CGAM= 2.929000E-01(∓0.      )

AREA= 6.090363E+00

PHI1= 8.57916223E-06      PHI2= 3.79343285E-03      PHI1/PHI2= 2.26158273E-03
```

The results are shown in figure 8.

REFERENCES

1. Debrunner, P.; and Frauenfelder, H.: Mössbauer Scattering. Applications of the Mössbauer Effect in Chemistry and Solid-State Physics, Tech. Rep. Ser. No. 50, Int. At. Energy Agency, 1966, pp. 58-73.

2. Ord, R. N.: A Mössbauer Resonance Effect Study Using a Backscatter Geometry. Appl. Phys. Lett., vol. 15, no. 9, Nov. 1, 1969, pp. 279-282.

3. Hershkowitz, N.; and Walker, J. C.: Mössbauer Scattering With Efficient Geometry. Nucl. Instrum. & Methods, vol. 53, no. 2, Aug. 1967, pp. 273-276.

4. Spijkerman, J. J.; Travis, J. C.; Pella, P. A.; and DeVoe, J. R.: Preliminary Study on the Characteristics and Design Parameters for a Mössbauer Resonant Detector. NBS Tech. Note 541, U.S. Dep. Com., Jan. 1971.

5. Lackner, Helmut G.: The Mössbauer Effect and Its Application to Measuring Technology. Aerospace Measurement Techniques, Gene G. Mannella, ed., NASA SP-132, 1967, pp. 1-27.

6. Netusil, W. F.; and Witherspoon, J. E.: Small Amplitude Vibration Calibration Using the Mossbauer Effect. Nucleonics in Aerospace, Paul Polishuk, ed., Plenum Press, Inc., 1968, pp. 65-79.

7. Muir, Arthur H., Jr.; Ando, Ken J.; and Coogan, Helen M.: Mössbauer Effect Data Index 1958-1965. Interscience Publ., 1966.

8. Howser, Lona M.; Singh, Jag J.; and Smith, Robert E., Jr.: A Computer Program for Mössbauer Data Processing. NASA TM X-2522, 1972.

TABLE I.- COMPARISON BETWEEN THE CALCULATED AND MÖSSBAUER COMPUTED VALUES OF THE SCATTERER VELOCITIES

Sinusoidal scatterer velocity		Constant scatterer velocity	
Directly calculated values, mm/sec (a)	Computed values, mm/sec	Directly measured values, mm/sec (b)	Computed values, mm/sec
±(0.467 ± 0.010)	±(0.487 ± 0.015)	±(0.500 ± 0.005)	±(0.497 ± 0.008)
±(0.701 ± 0.010)	±(0.719 ± 0.012)	±(1.000 ± 0.010)	±(1.003 ± 0.011)
±(0.939 ± 0.010)	±(0.957 ± 0.012)	±(1.500 ± 0.015)	±(1.501 ± 0.015)
±(1.158 ± 0.010)	±(1.126 ± 0.015)	±(2.000 ± 0.020)	±(1.979 ± 0.014)
±(1.401 ± 0.010)	±(1.382 ± 0.014)	±(2.500 ± 0.025)	±(2.501 ± 0.011)
±(1.635 ± 0.010)	±(1.630 ± 0.016)	±(3.000 ± 0.030)	±(3.023 ± 0.020)
±(1.864 ± 0.010)	±(1.820 ± 0.017)		
±(2.098 ± 0.010)	±(2.076 ± 0.021)		
±(2.339 ± 0.010)	±(2.377 ± 0.019)		

[a] The errors on directly calculated values include the combined effect of errors on a_o and ω in the expression, $V_{max} = a_o\omega$. (a_o and ω represent the amplitude and the angular velocity of the scatterer motion, respectively.)

[b] The errors on these values represent the calibration accuracy of the constant-velocity values of the scatterer drive system (namely, 1 percent of the velocity scale setting).

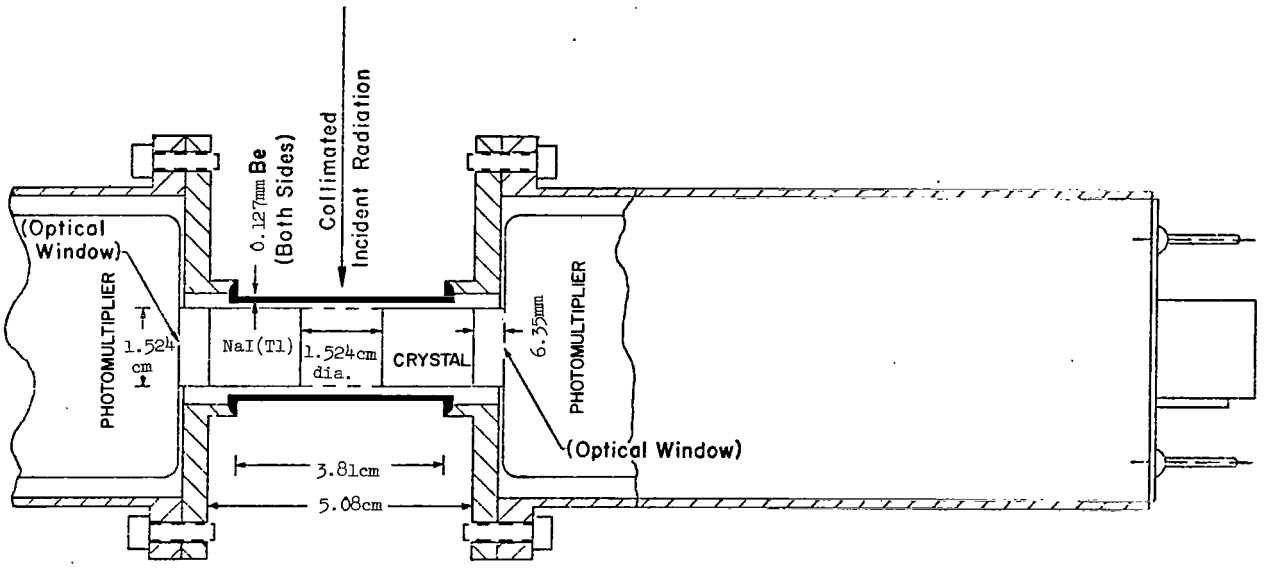

Figure 1.- Schematic drawing of the annular NaI(Tl) detector assembly. (Notice the beryllium windows on both sides.)

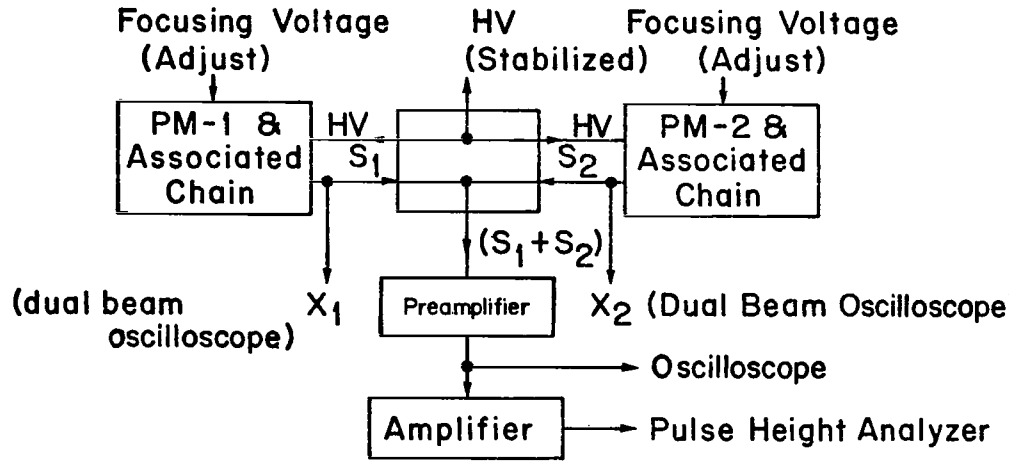

(a) General circuit for equalizing photomultiplier gains and pulse arrival times.

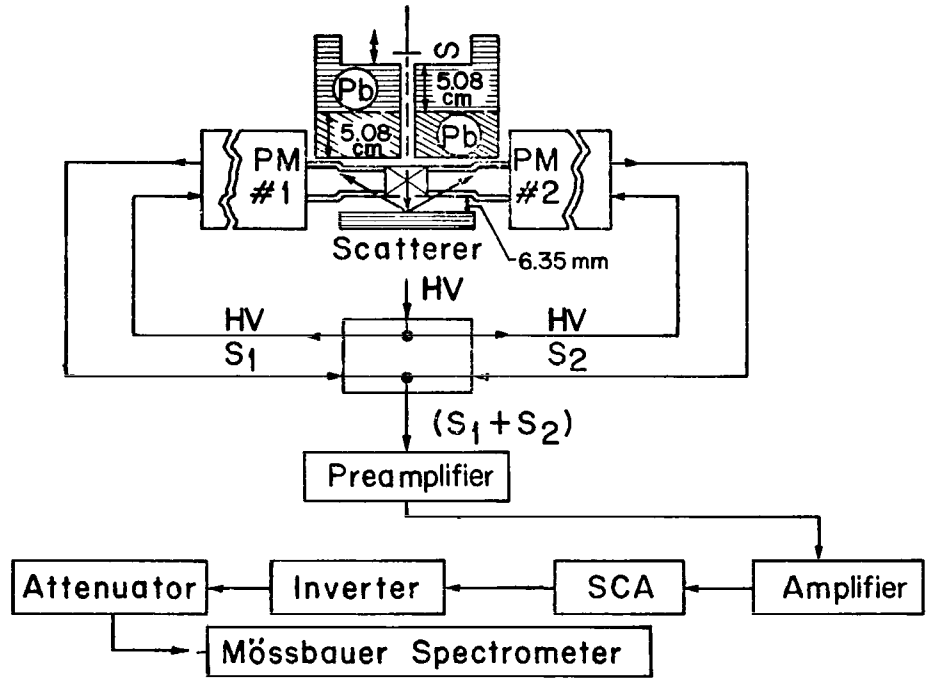

(b) Schematic diagram of the signal conditioning circuit for Mössbauer spectrometer.

Figure 2.- Simplified diagram of the electronic circuit.

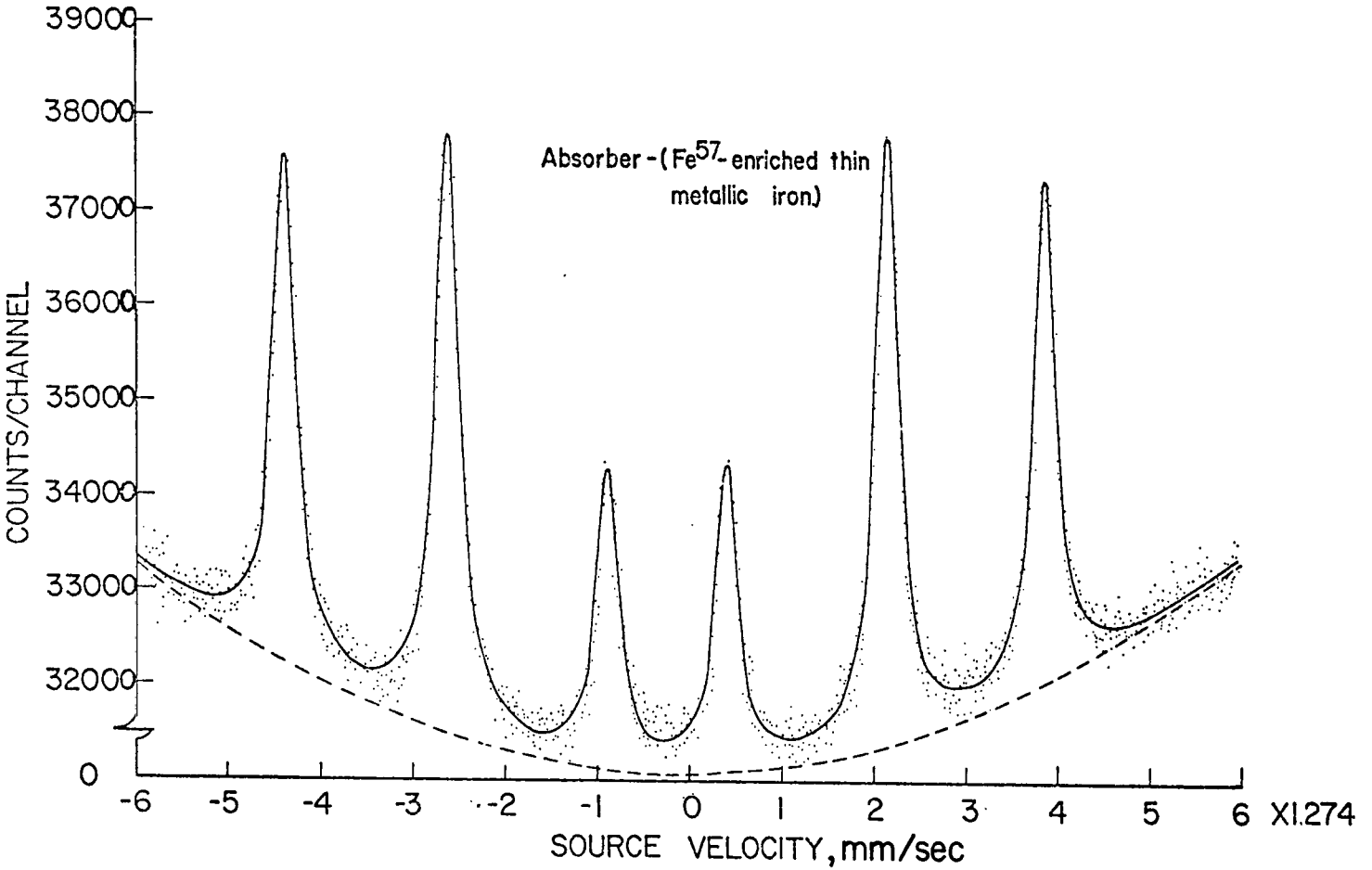

Figure 3.- A typical transmission spectrum from a thin (0.8 mg/cm2) Fe^{57}-enriched iron absorber with the detector described in this paper. (Notice the characteristic scattering peaks instead of the transmission dips.)

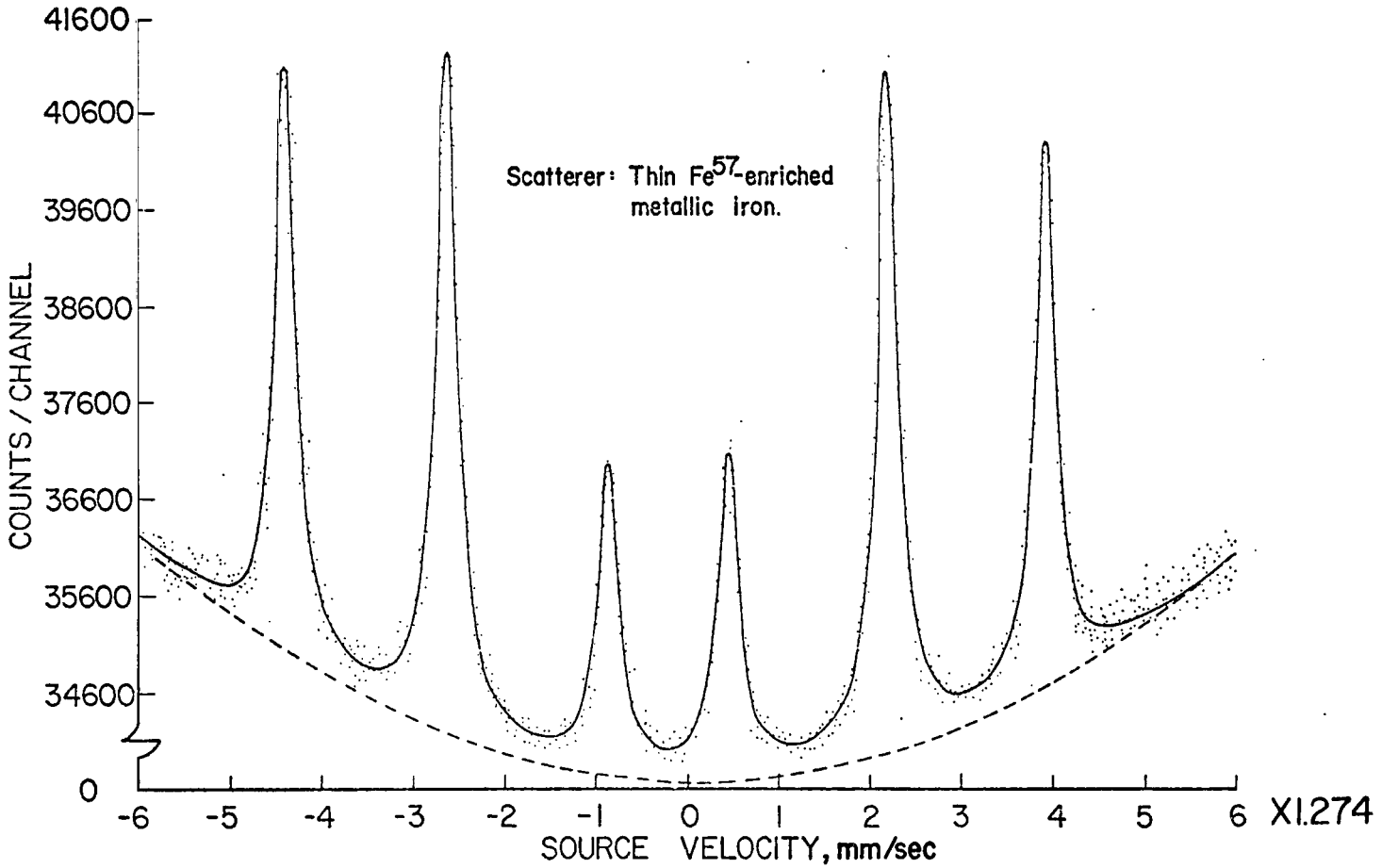

Figure 4.- A typical backscattering spectrum from a thin (0.8 mg/cm^2) Fe^{57}-enriched iron scatterer with the detector described in this paper. (Notice the pronounced scattering peaks characteristic of scattering geometry.)

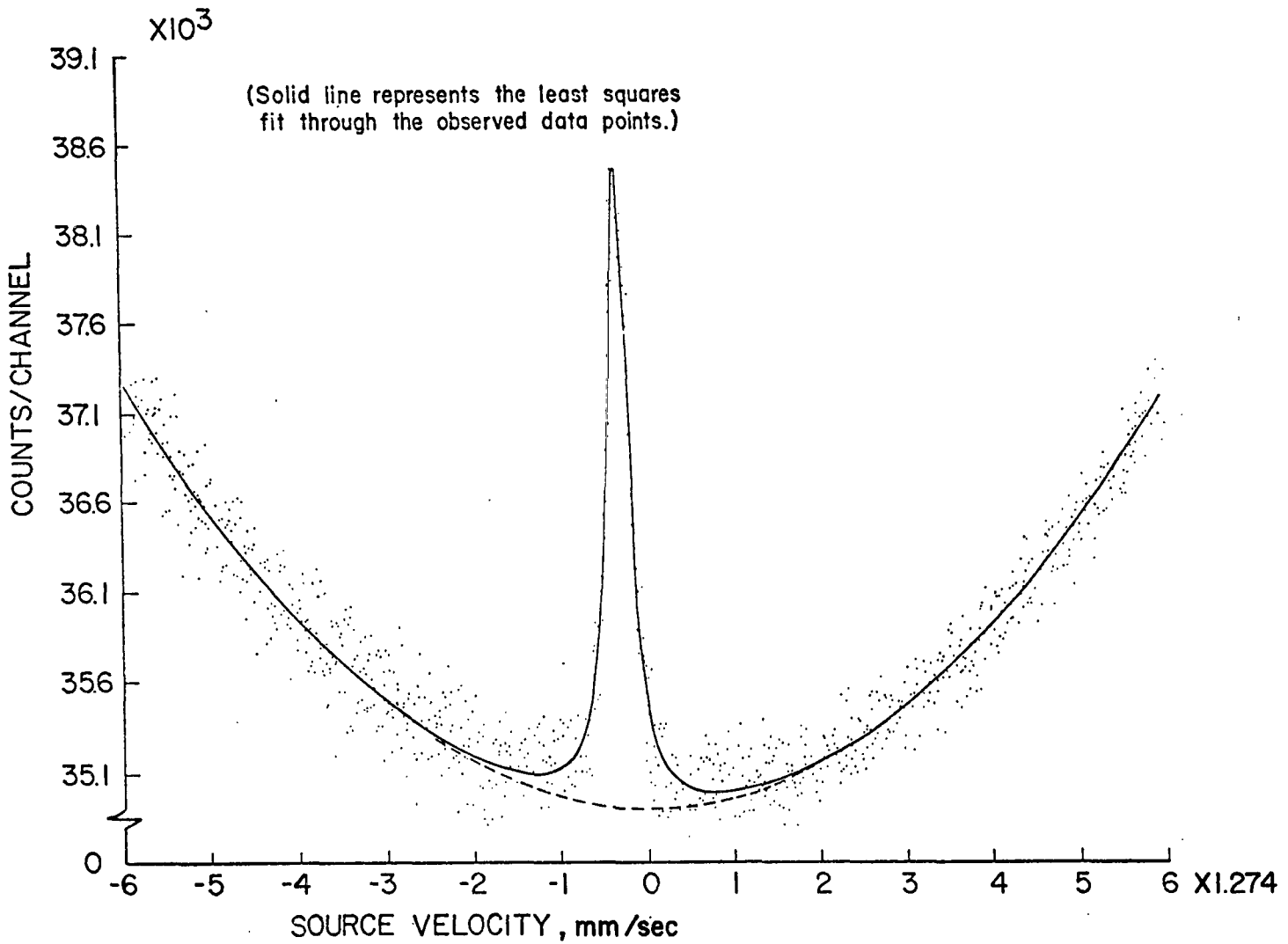

Figure 5.- Backscattered spectrum from a stainless steel (type 347) specimen using the radiation detector described in this paper.

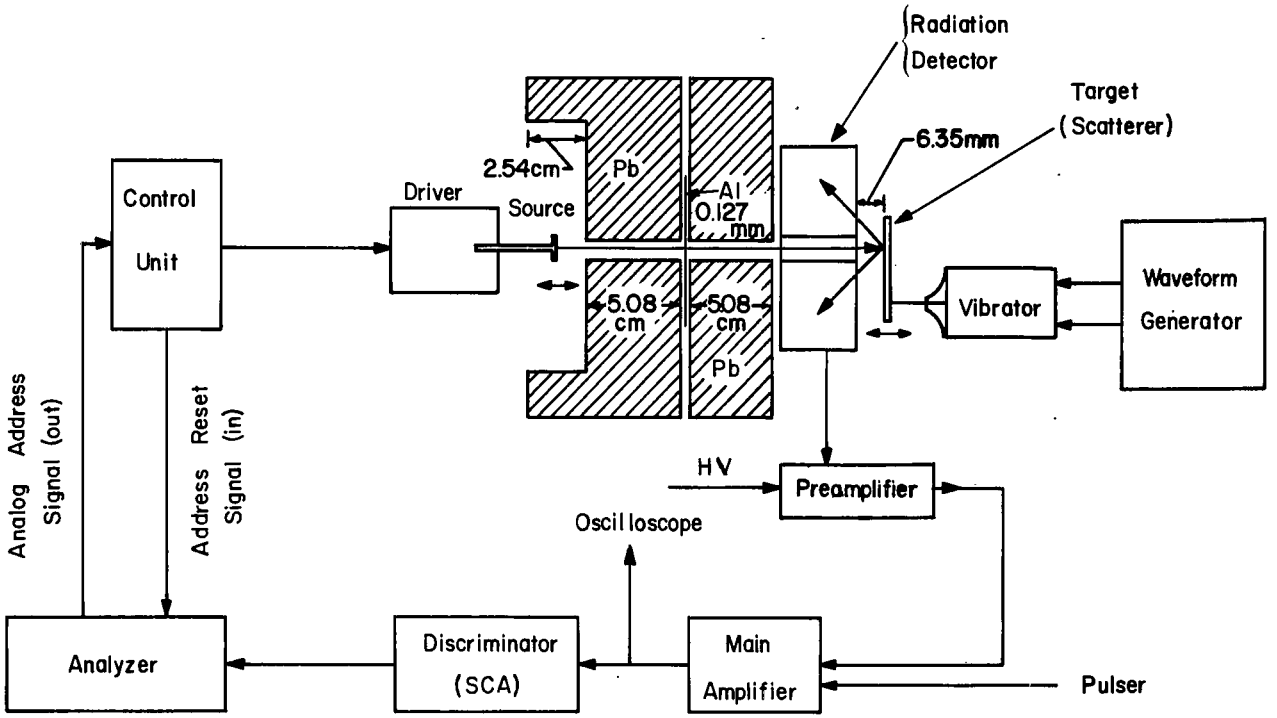

Figure 6.- Schematic diagram of the experimental setup used in this study.

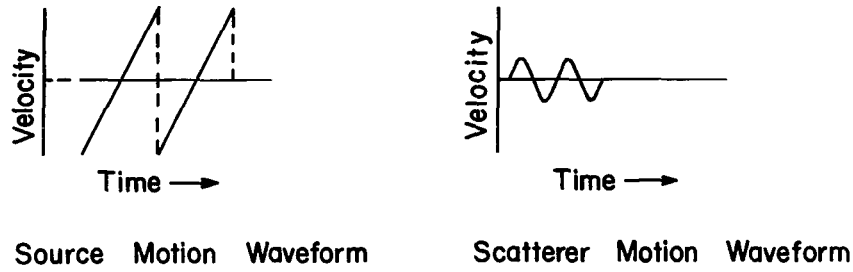

(a) Sinusoidal scatterer motion.

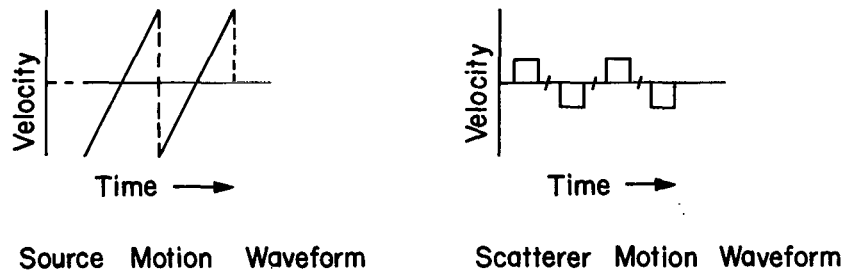

(b) Constant-velocity scatterer motion.

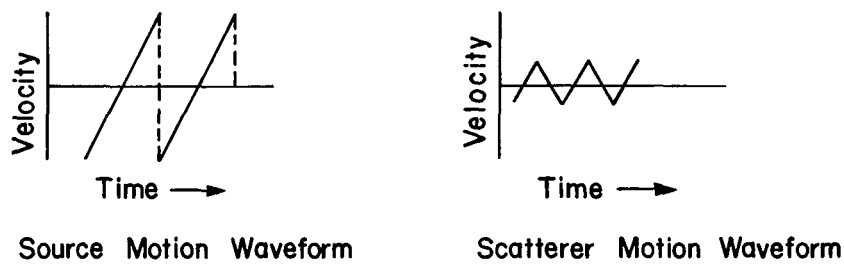

(c) Constant-acceleration scatterer motion.

Figure 7.- Summary of source-scatterer motions.

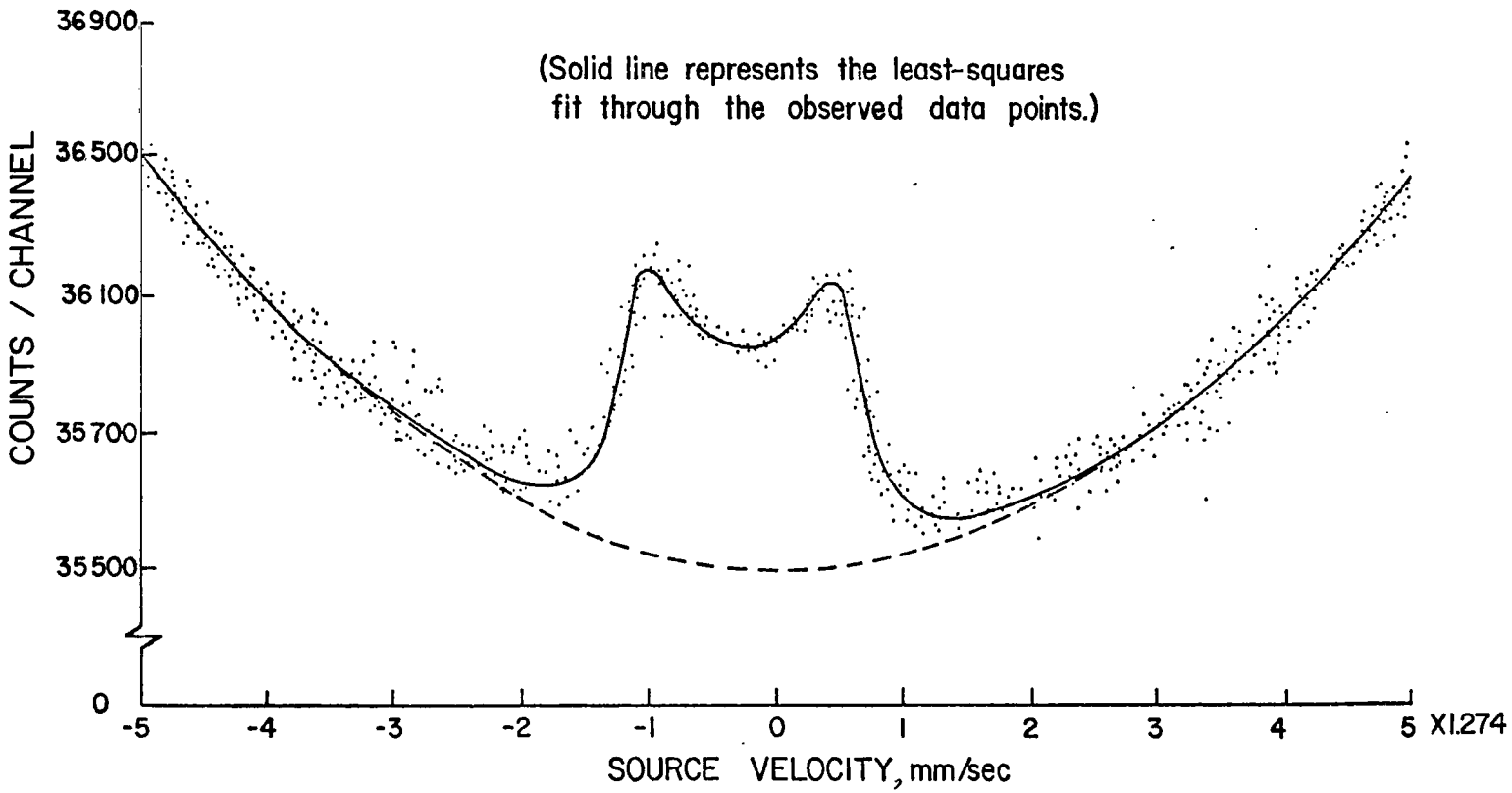

Figure 8.- Typical Mössbauer spectrum obtained when the source and the scatterer were in random relative motion. The source was moving with a constant acceleration when the stainless steel (type 347) scatterer was subjected to a sinusoidal motion.

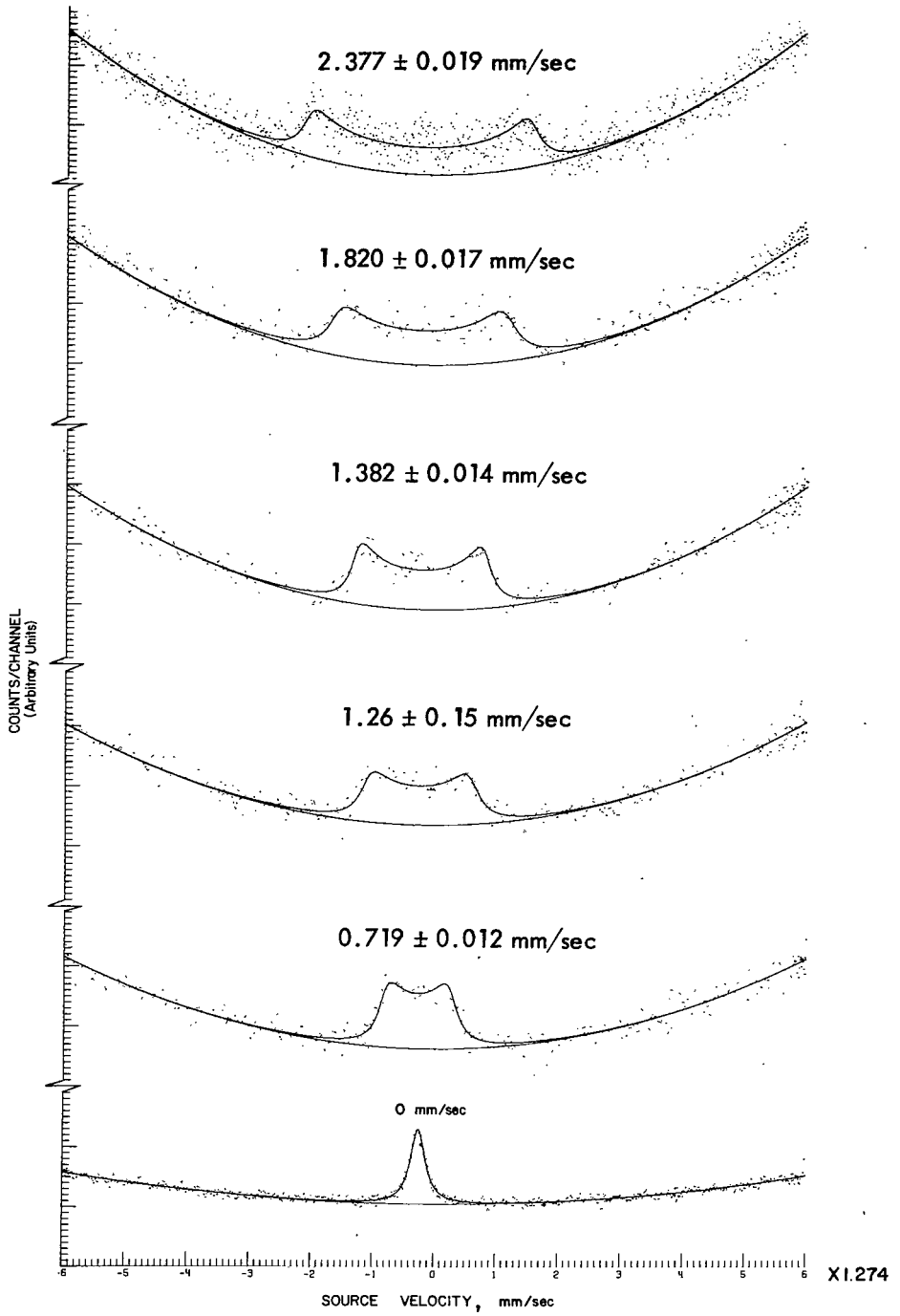

Figure 9.- Mössbauer spectra from stainless steel (type 347) scatterers moving with different sinusoidal velocities. The numbers on each graph indicate maximum scatterer velocities.

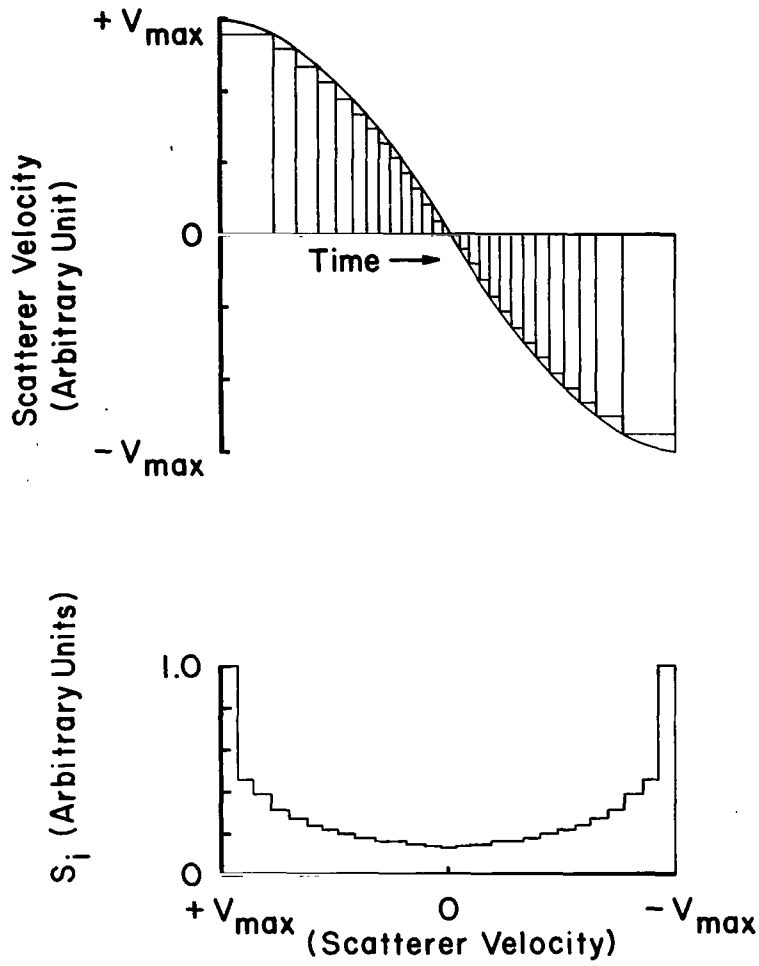

Figure 10.- Numerical calculation of S_i for sinusoidal scatterer motion. (The number of velocity subdivisions shown in this figure is arbitrary and is for the purpose of illustration only.)

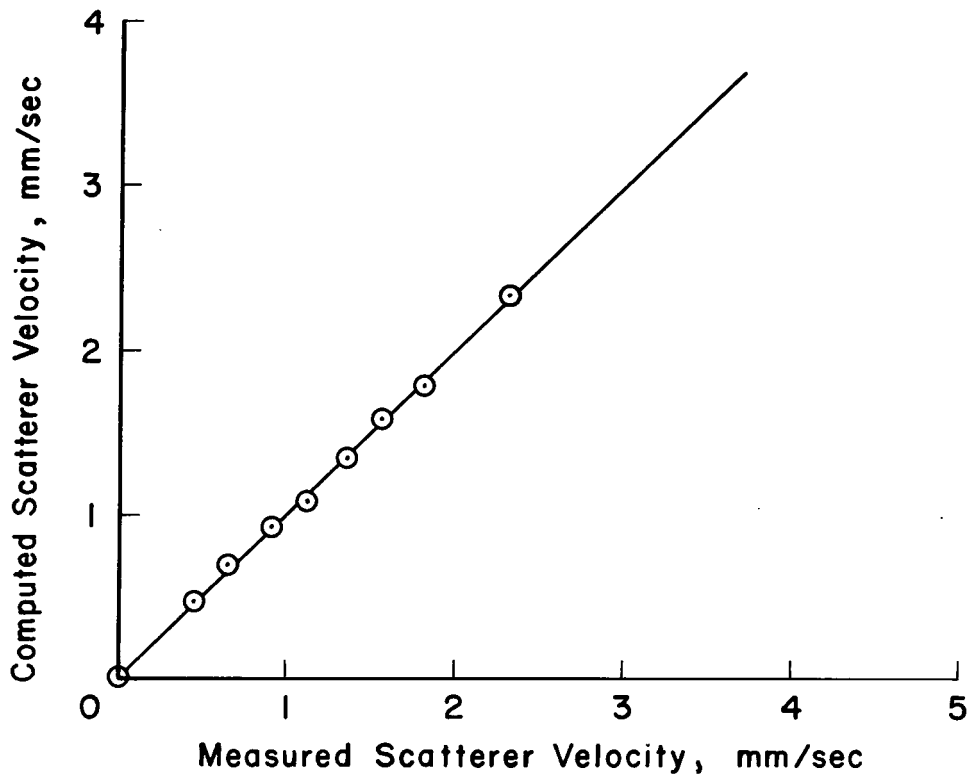

Figure 11.- Comparison between the directly calculated and the Mössbauer computed values of V_{max}. (The line represents points of exact equality.)

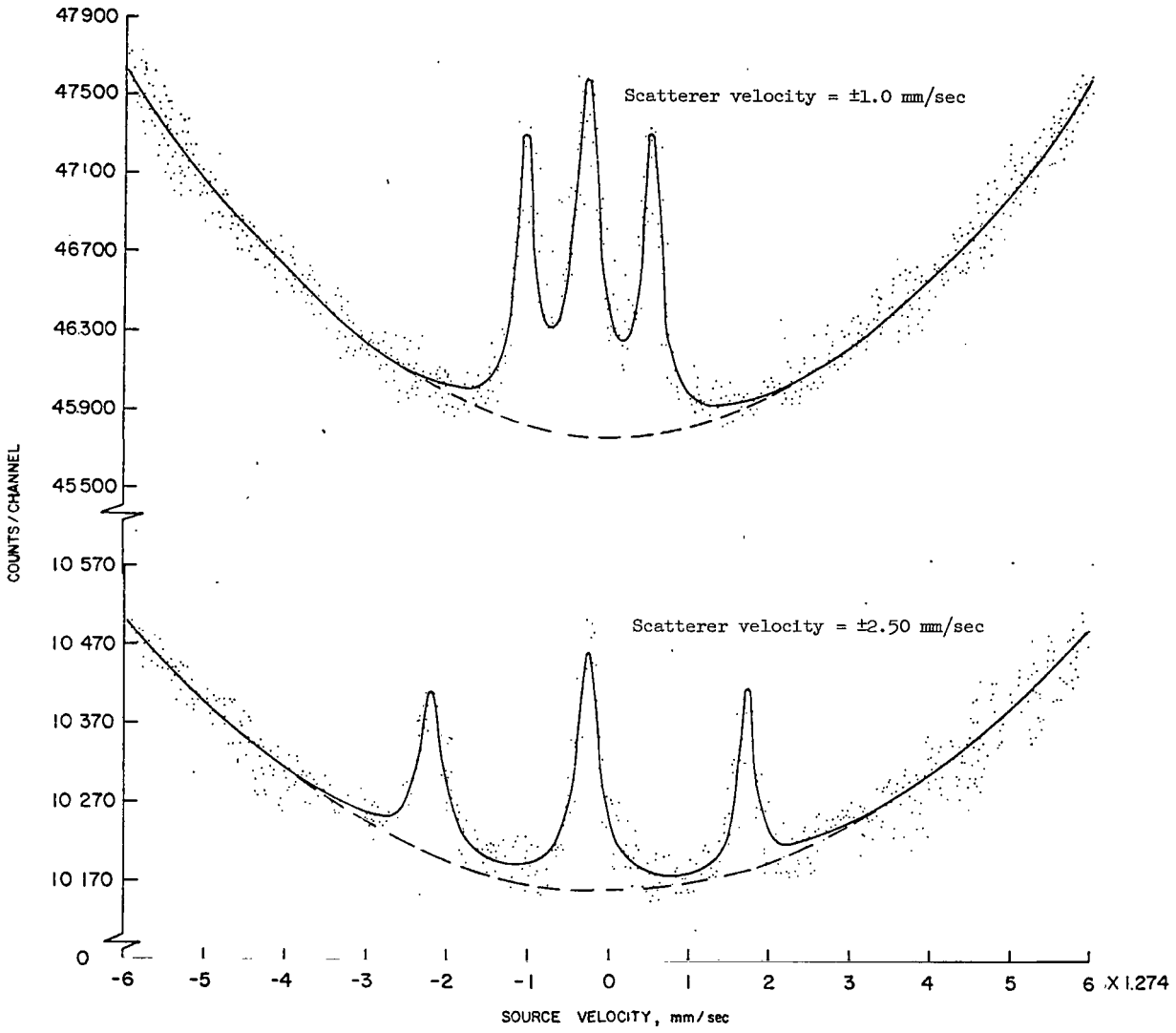

Figure 12.- Typical backscattered Mössbauer spectra from a 0.762-cm thick stainless steel (type 347) scatterer moving with constant velocity. The Co^{57}-source had a constant-acceleration motion of ±6(1.274) mm/sec. (There was no phase correlation between the source and scatterer motions.)

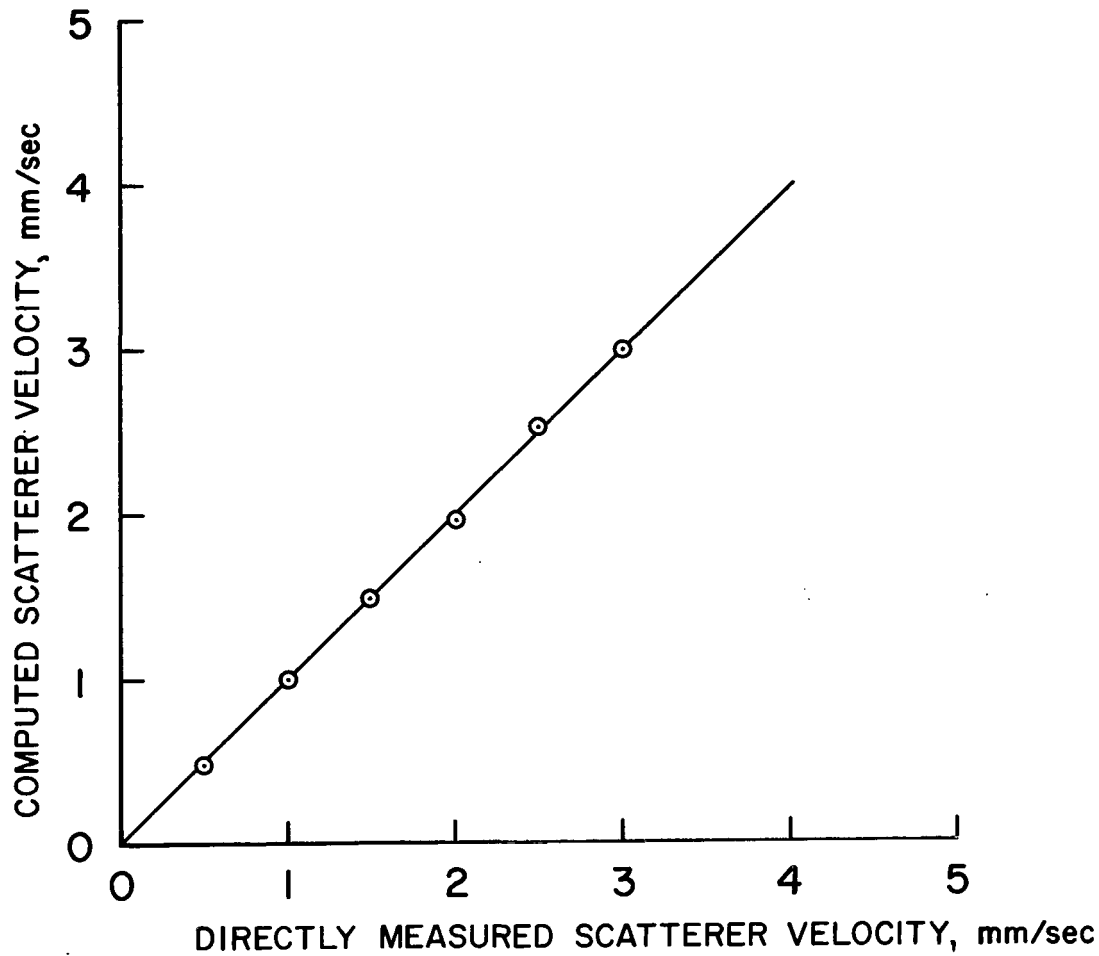

Figure 13.- Comparison between the computed and directly measured values of scatterer velocity. The scatterer motion was of constant-velocity type and had random phase with respect to constant acceleration motion of the source.

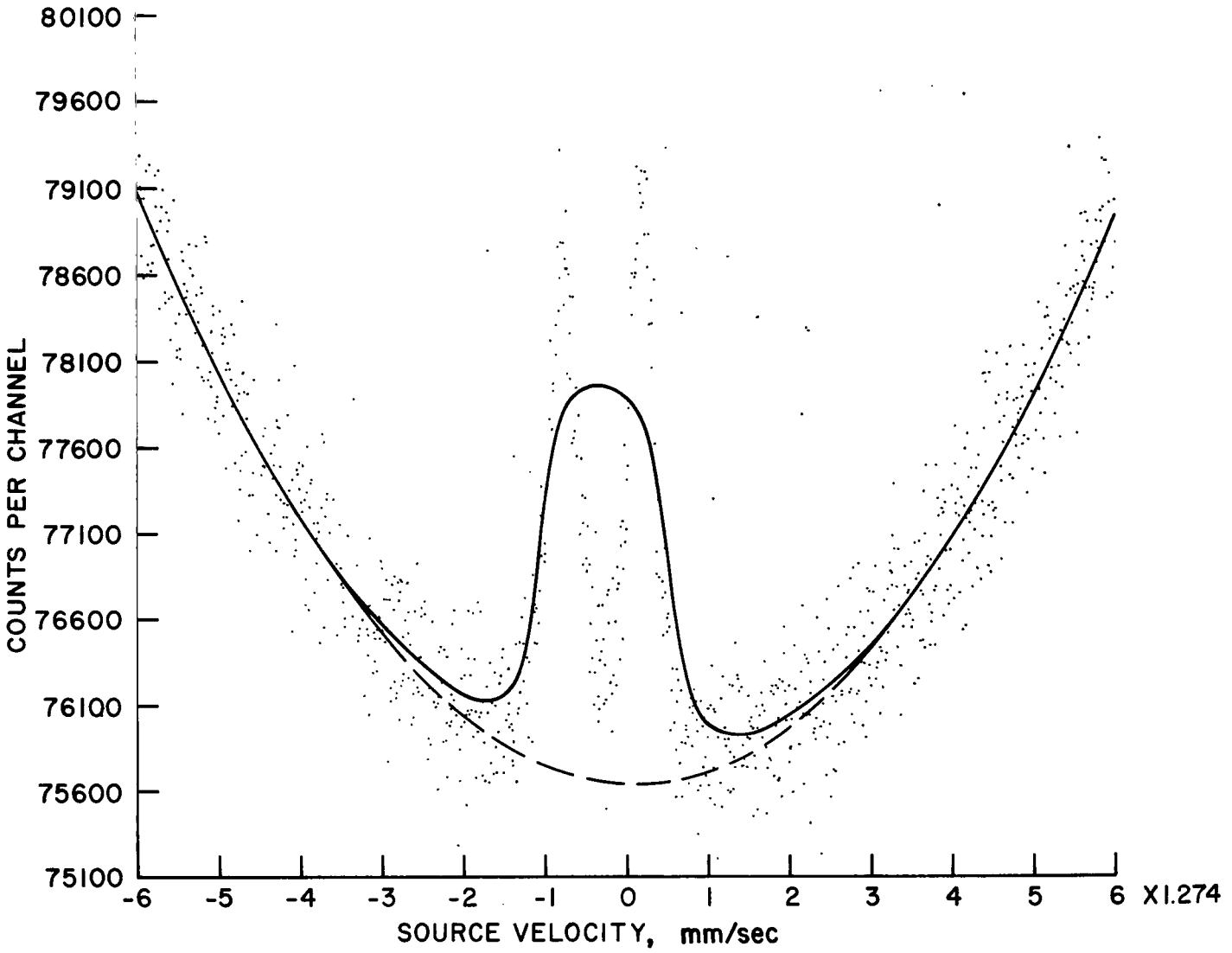

Figure 14.- Experimental Mössbauer spectrum observed from a stainless steel (type 347) scatterer moving with constant-acceleration motion. The solid line shows a theoretically predicted spectrum under these conditions.

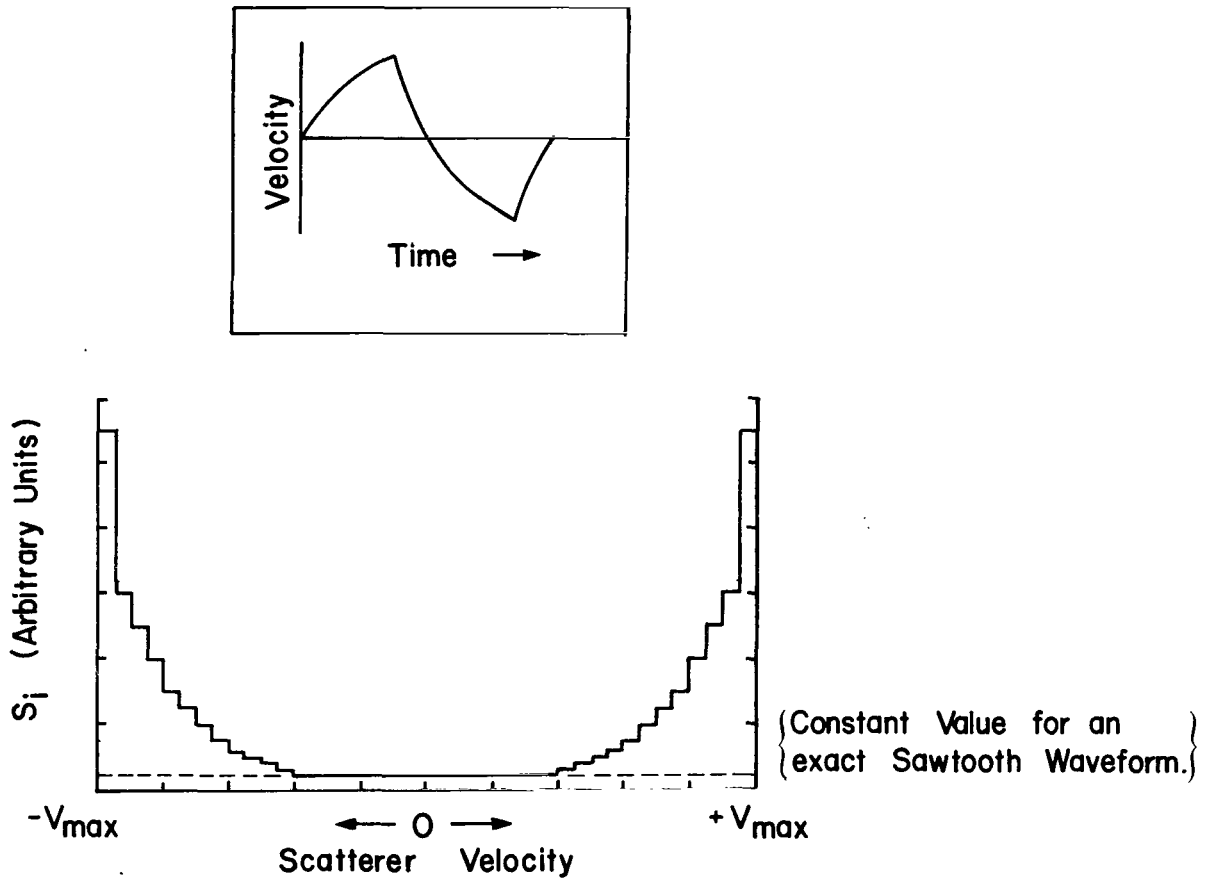

Figure 15.- Relative dwell times S_i for the experimental waveform of the scatterer motion (see insert) used to obtain the experimental spectrum shown in figure 14.

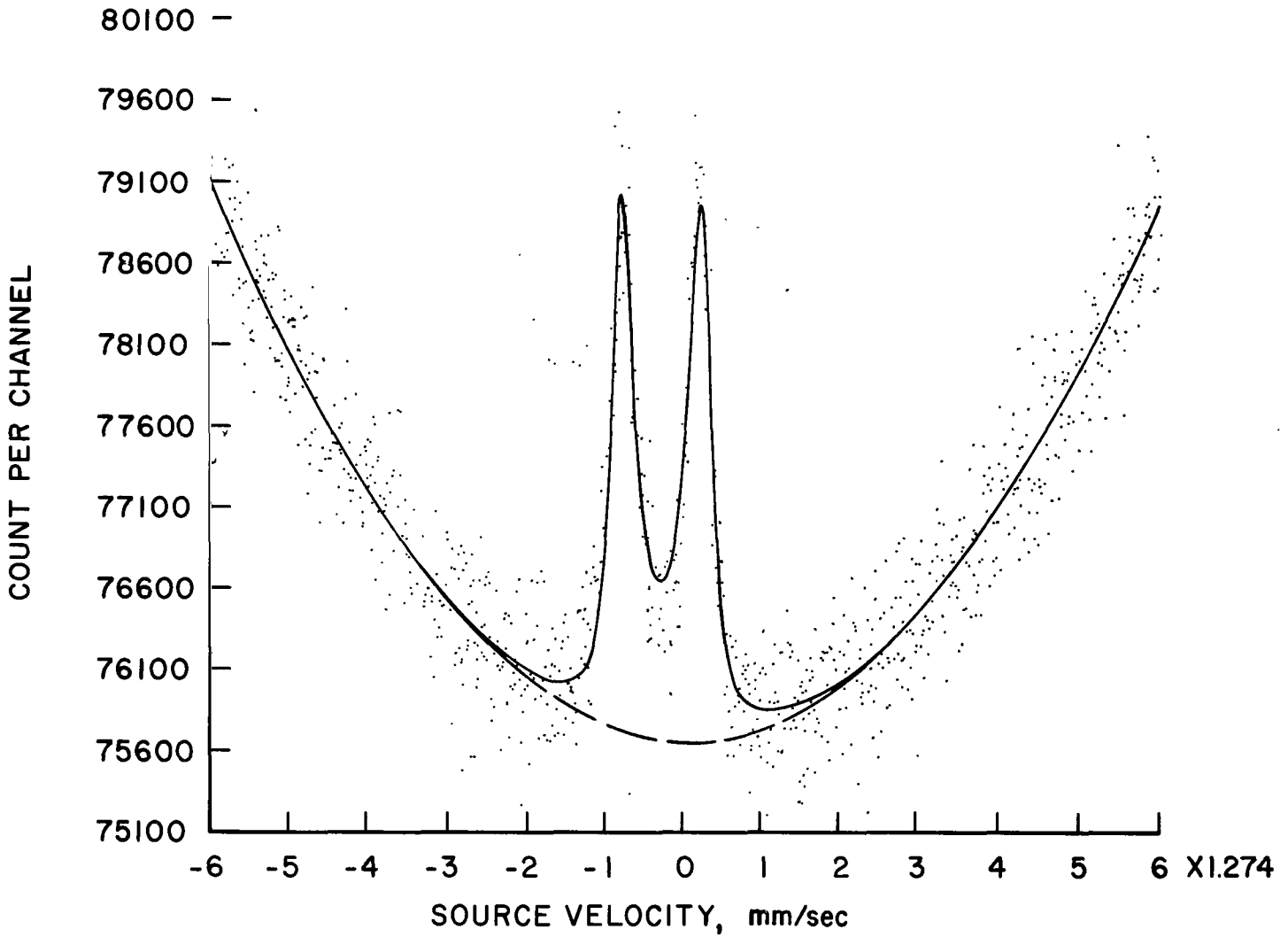

Figure 16.- Comparison between the experimental and the theoretical Mössbauer spectrum predicted on the basis of S_i values shown in figure 15.

SOURCE VELOCITY LIMITS = ± 6 (1.274) mm/sec

SCATTERER VELOCITY LIMITS = ± 2 (1.274) mm/sec

THE SOLID LINE REPRESENTS THE EFFECT OF THE SCATTERER MOTION SUPERIMPOSED ON BASE-LINE PARABOLA.

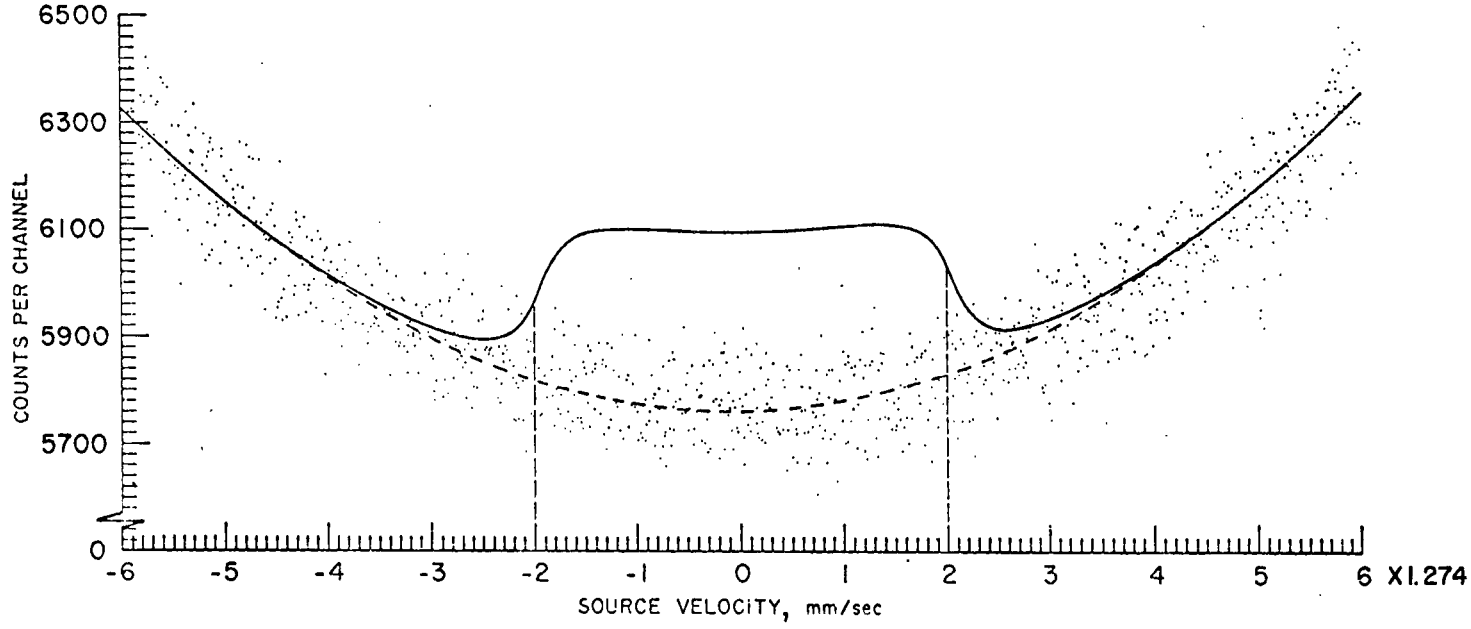

Figure 17.- Computed backscattered Mössbauer spectrum from a nonmagnetic steel scatterer subjected to a true constant-acceleration motion at the same time when the source was also moving with constant-acceleration motion.

"The aeronautical and space activities of the United States shall be conducted so as to contribute . . . to the expansion of human knowledge of phenomena in the atmosphere and space. The Administration shall provide for the widest practicable and appropriate dissemination of information concerning its activities and the results thereof."

— NATIONAL AERONAUTICS AND SPACE ACT OF 1958

NASA SCIENTIFIC AND TECHNICAL PUBLICATIONS

TECHNICAL REPORTS: Scientific and technical information considered important, complete, and a lasting contribution to existing knowledge.

TECHNICAL NOTES: Information less broad in scope but nevertheless of importance as a contribution to existing knowledge.

TECHNICAL MEMORANDUMS: Information receiving limited distribution because of preliminary data, security classification, or other reasons.

CONTRACTOR REPORTS: Scientific and technical information generated under a NASA contract or grant and considered an important contribution to existing knowledge.

TECHNICAL TRANSLATIONS: Information published in a foreign language considered to merit NASA distribution in English.

SPECIAL PUBLICATIONS: Information derived from or of value to NASA activities. Publications include conference proceedings, monographs, data compilations, handbooks, sourcebooks, and special bibliographies.

TECHNOLOGY UTILIZATION PUBLICATIONS: Information on technology used by NASA that may be of particular interest in commercial and other non-aerospace applications. Publications include Tech Briefs, Technology Utilization Reports and Technology Surveys.

Details on the availability of these publications may be obtained from:

SCIENTIFIC AND TECHNICAL INFORMATION OFFICE

NATIONAL AERONAUTICS AND SPACE ADMINISTRATION

Washington, D.C. 20546